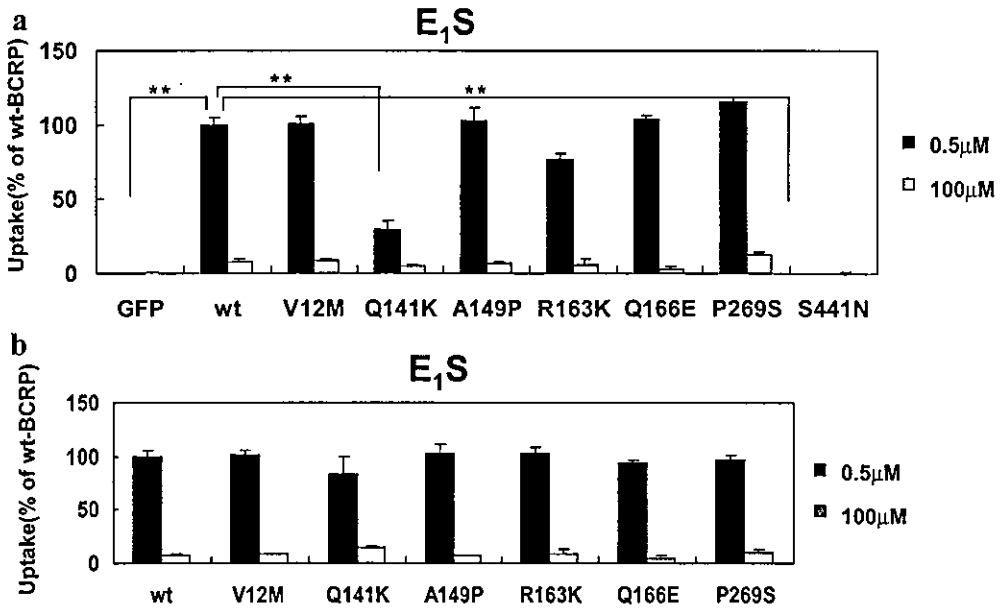

Fig. 3. The transport of E_1S by BCRP variants. The uptake of [^{3}H]E_1S by 2 μg membrane vesicles prepared from BCRP cDNA-infected and GFP cDNA-infected HEK 293 cells was examined for 2 min at 37°C in a medium containing 33 nM [^{3}H]labeled E_1S, tracer (0.5 μM) and excess concentrations (100 μM) of unlabeled E_1S. Panel 3a shows the ATP-dependent uptake of [^{3}H]E_1S by BCRP variants after normalization by the membrane protein level. The uptake was calculated by subtracting the ligand uptake in the absence of ATP from that in its presence. Panel 3b shows the ATP-dependent uptake of [^{3}H]E_1S by BCRP variants after normalization by the BCRP protein levels. For the preparation of Panel 3b, the data in Panel 3a were corrected by taking into account the BCRP protein expression level in each membrane vesicle preparation determined by the Western blot analysis (Fig. 2). Results are given as % of the wild-type BCRP. **Significantly different from wild type BCRP-expressing membrane vesicles by ANOVA followed by Dunnett's test ($p < 0.01$).

transport activity. BCRP expression systems were constructed using recombinant adenoviruses with the expectation of the high expression of the exogenous genes. Compared with the membrane vesicles isolated form the P-388 cells which were infected with BCRP cDNA by the recombinant retroviruses (11), the uptake of E_1S per mg membrane protein determined in the present study was much higher. This expression system may be useful for the analysis of functional changes in SNP variants of BCRP in a sensitive manner.

Our findings suggest that two SNP variants of BCRP may affect the function of BCRP. Q141K BCRP showed a lower expression level, which is approximately 30–40% of that of the wild type. This result is consistent with the previous report that the transfection of Q141K BCRP cDNA to PA317 cells and KB-3-1 human cells also resulted in lower expression levels (19). Recently, investigation of the expression level of BCRP in 99 Japanese placenta samples revealed that people who were homozygous for this mutation showed significantly lower expression levels of BCRP (D. Kobayashi, I. Ieiri, H. Takane, M. Kimura, Y. Norikawa, H. Tohyama, S. Irie, A. Urae, H. Suzuki, H. Kusuhara, N. Terakawa, K. Mine, K. Ohtsubo and Y. Sugiyama, data presented at 18th Annual Meeting of The Japanese Society for the Study of Xenobiotics, Sapporo, October 8–10, 2003). The clinical relevance of this *in vitro* study has major implications from the point of view of the utility of the *in vitro* system for the prediction of individual pharmacokinetic difference.

Although more detailed analysis is required to clarify the mechanism governing the reduced protein expression of Q141K BCRP, immunohistochemical staining revealed that this variant is expressed on the plasma membrane and, therefore, the altered cellular localization may not be related to the reduced protein level. It has been reported that the mRNA level of this variant is similar to that of the wild type in the transfected cells where the reduced protein level was observed (19). In addition, in the human intestine, the expression of BCRP mRNA was similar in subjects with wild type and Q141K BCRP genes, whereas there was no significant correlation between the protein and mRNA levels for BCRP (20). It has also been suggested that linkage disequilibrium is present between a CTCA deletion in the 5′-flanking region (g-19572-19569) and Q141K in Swedish subjects (21). More detailed analysis is required to clarify the mechanism for the reduced protein expression of this BCRP variant and its physiologic significance.

As far as the cellular localization was concerned, S441N BCRP was the only variant which was expressed in the intracellular compartment. We also found that the intracellular localization of S441N BCRP in HEK293 cells after transient expression (data not shown), whereas the wild-type BCRP was expressed on the cell membrane. It is possible that this variant is retained in the endoplasmic reticulum and most of the protein is degraded in the proteosomes as reported for many kinds of membrane proteins (22). Western blot analysis revealed that the expression of S441N is significantly lower than the wild type BCRP. Its expression level was reduced not only in the isolated membrane fraction, but also in the whole cell lysate (Fig. 2). These results suggest that this SNPs may

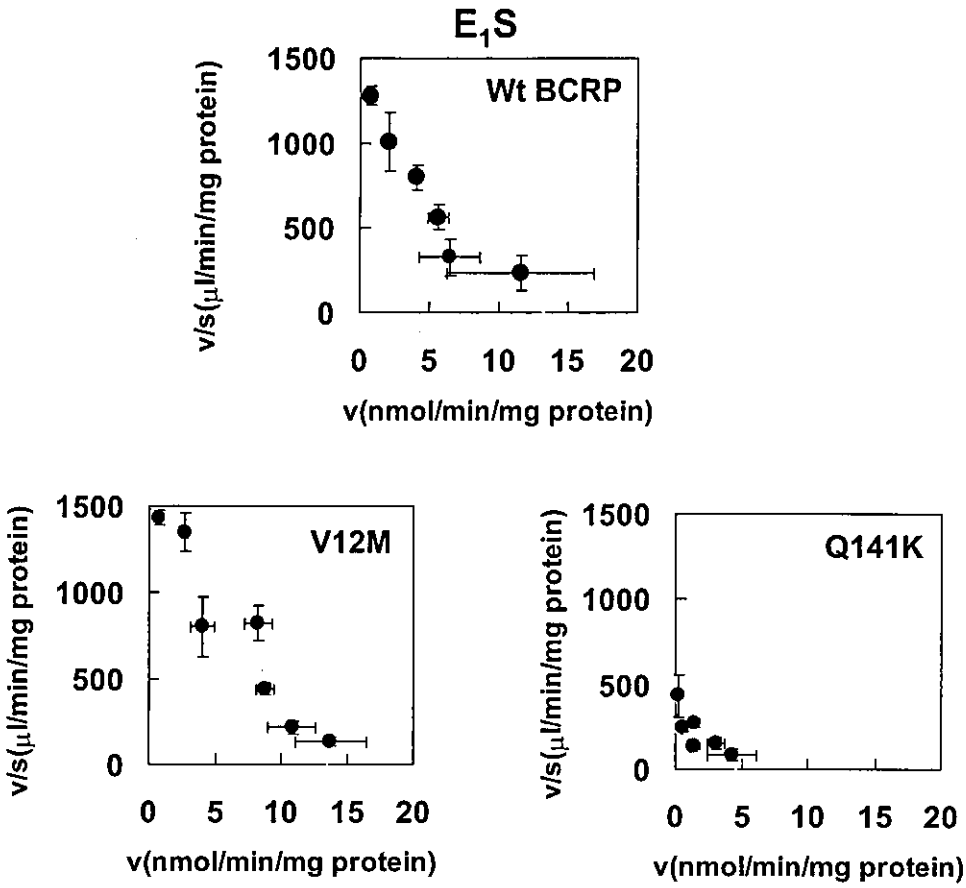

Fig. 4. Saturation of BCRP mediated transport of E_1S. Saturation of [^{3}H]E_1S transport was determined for the wild-type, V12M, and Q141K BCRP. The uptake of [^{3}H]E_1S by 2 μg membrane vesicles prepared from BCRP cDNA-infected HEK 293 cells was examined for 1 min at 37°C in a medium containing 33 nM [^{3}H]labeled E_1S and several concentrations of unlabeled E_1S. The results are given as the Eadie-Hofstee plots. Each point and bar represents the mean ± SE value of triplicate determinations.

affect both cellular localization and expression level. Concerning the cellular localization of SNPs variants of BCrP, Mizuarai *et al.* reported the intracellular localization of V12M BCRP in stably transfected LLC-PK1 cells very recently (23). The finding by Mizuarai *et al.* (23) was in marked contrast to the present finding that V12M BCRP is expressed on the apical membrane of transiently transfected LLC-PK1 cells (Fig. 1). At the present moment, we do not have any good answer to account for the discrepancy. It is possible that the cellular localization of V12M BCRP is affected by the culture conditions of LLC-PK1 cells.

Although it has been reported that the amino acid replacement at the protein of 482 alters the substrate specificity of BCRP (12,13), there has been no report on alterations in the substrate specificity due to SNP variations. In the present study, we examined the transport activity of some organic anions using isolated membrane vesicles expressing the wild type and SNP variants of BCRP. In addition to the previously described substrates such as E_1S, DHEAS and methotrexate (11), we found that PAH is also transported by BCRP. For these compounds, our results indicated that the transport activity per BCRP molecule for 6 kinds of SNP variants (V12M, A149P, R163K, Q166E, P269S, and also Q141K BCRP) is almost the same as that of the wild type BCRP (Figs. 3 and 5). In addition, the extent of the inhibition of the transport of [^{3}H]DHEAS, [^{3}H]methotrexate and [^{3}H]PAH by 80 μM DHEAS, 450 μM methtrexate and 3 mM PAH, respectively (Fig. 5), is accounted for by considering the transport char-

Fig. 5. The transport of DHEAS, MTX, and PAH by BCRP variants. The uptake of each compounds by 10 μg membrane vesicles prepared from BCRP and GFP expressing-HEK 293 cells was examined for 2 min at 37°C in a medium containing 33 nM [^{3}H]labeled compounds, tracer (0.5 μM), and excess concentrations (80 μM, 450 μM, and 3 mM, for DHEAS, MTX, and PAH, respectively) of unlabeled compounds. Panel 5a shows the ATP-dependent uptake of [^{3}H]compounds by BCRP variants after normalization by the membrane protein level. The uptake was calculated by subtracting the ligand uptake in the absence of ATP from that in its presence. Panel 5b shows the ATP-dependent uptake of these compounds by BCRP variants after normalization by the BCRP protein levels. For the preparation of Panel 5b, the uptake data were corrected by taking into account the BCRP protein expression level in each membrane vesicle preparation determined by the Western blot analysis (Fig. 2). Results are given as % of the wild type BCRP. **Significantly different from the wild type BCRP-expressing membrane vesicles by ANOVA followed by Dunnett's test ($p < 0.01$).

a

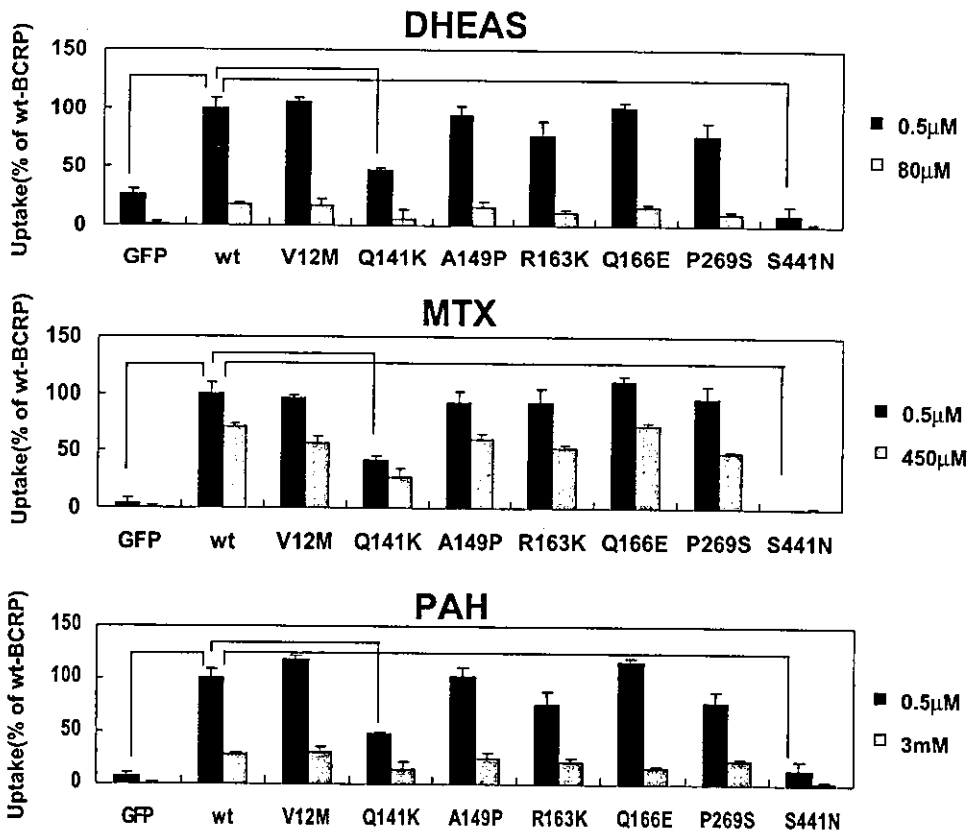
DHEAS
Uptake(% of wt-BCRP)
150
100
50
0
GFP wt V12M Q141K A149P R163K Q166E P269S S441N
0.5μM
80μM
MTX
Uptake(% of wt-BCRP)
150
100
50
0
GFP wt V12M Q141K A149P R163K Q166E P269S S441N
0.5μM
450μM
PAH
Uptake(% of wt-BCRP)
150
100
50
0
GFP wt V12M Q141K A149P R163K Q166E P269S S441N
0.5μM
3mM

b

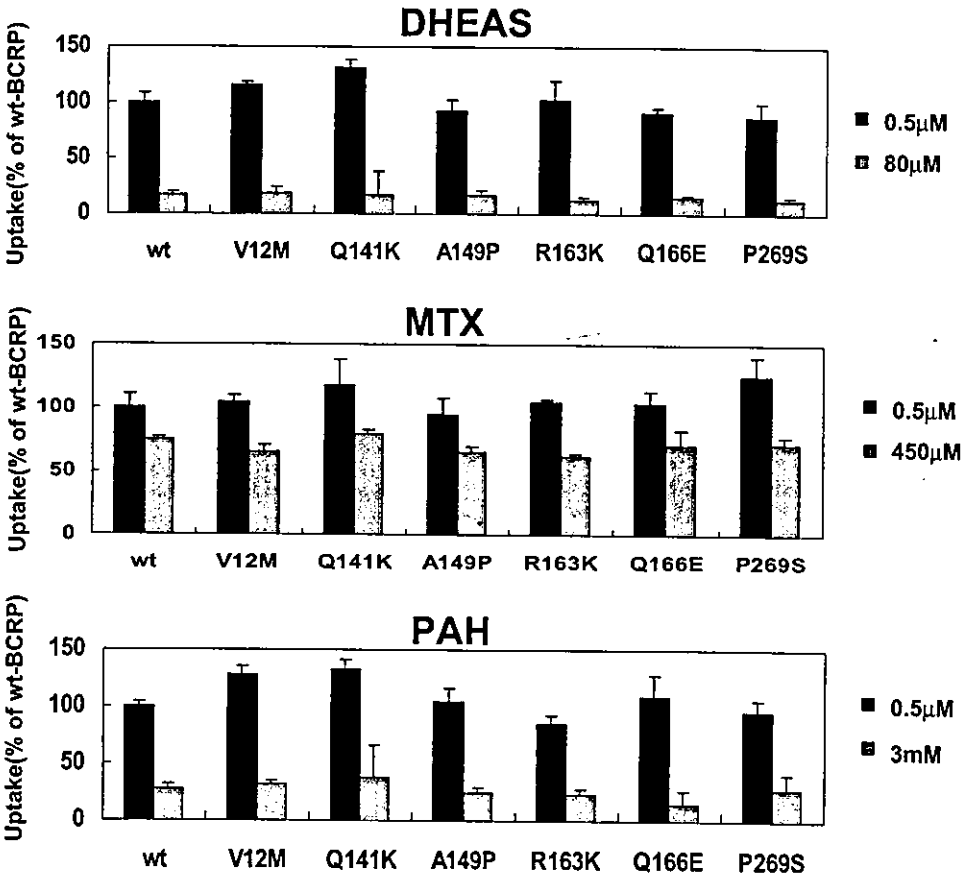
DHEAS
Uptake(% of wt-BCRP)
150
100
50
0
wt V12M Q141K A149P R163K Q166E P269S
0.5μM
80μM
MTX
Uptake(% of wt-BCRP)
150
100
50
0
wt V12M Q141K A149P R163K Q166E P269S
0.5μM
450μM
PAH
Uptake(% of wt-BCRP)
150
100
50
0
wt V12M Q141K A149P R163K Q166E P269S
0.5μM
3mM

acteristics of these compounds; we reported that DHEAS reduced the BCRP-mediated transport of [^{3}H]E_1S with an approximate IC_{50} value of 55 μM (11). The K_m value for BCRP-mediated transport of methotrexate is reported to be 0.68 ~1.34 mM (24,25). We also found that PAH is transported by BCRP with the K_m value of 3~5 mM (unpublished observations). Furthermore, the K_m values for E_1S were similar between the wild type, V12M and Q141K BCRP (Fig. 4).

It has been reported that there is a marked ethnic difference in the frequency of Q141K SNPs, and this is the prevalent allele in the Japanese population (19,21). In the present study, we constructed SNP variants of BCRP based on the information from 100 Japanese placenta specimens, 84 established cancer cell lines, and 60 Japanese individuals who received the administration of irinotecan. In particular, the frequency of the Q141K variant was 29~36% in the Japanese, whereas the frequency in 26 Caucasians subjects was only 8%. Among the 100 Japanese specimens, S441N SNPs were only found in one heterozygous subject and, consequently, their allele frequency was calculated to be only 0.5%. It is possible that the disposition of BCRP substrates is different between the subjects with the wild type BCRP and those with the SNPs variants of BCRP. One of the most important substrates for BCRP is pheophorbide a, a dietary catabolite of chlorophyll. It has been shown that the plasma concentration of pheophorbide a is increased in the Bcrp1 (−/−) mice, resulting in the occurrence of severe phototoxic ear lesions (10). Since pheophorbide a is also transported by human BCRP (10), it is likely that Q141K and S441N SNPs may be involved in the phototoxicity and protoporphyria induced by the intake of chlorophyll.

Concerning the disposition of antitumor drugs, it has also been reported that Bcrp1 (−/−) hematopoietic stem cells are sensitive to mitoxantrone-induced toxicity (26). These data suggest that the ability to protect stem cells from some genotoxic xenobiotics might be lower in subjects who have Q141K and S441N SNPs in BCRP gene. It has also been suggested that the oral absorption of topotecan is restricted by the intestinal expression of BCRP (9). This suggestion is based on the findings that, after the oral administration of both topotecan and the inhibitor of Mdr1 and Bcrp1, GF120918, the bioavailability of this antitumor drug in plasma was dramatically increased, not only in normal mice but also in Mdr1 (−/−) mice (9). It has also been reported that, in human jejunal biopsies, mRNA expression of BCRP is higher than that of MDR1 mRNA (27), suggesting the importance of BCRP in drug absorption. It has also been shown that BCRP plays an important role in placenta (9). In mdr1a/1b (−/−) mice, administration of GF120918 resulted in the higher topotecan levels in fetuses and maternal plasma. Moreover, SNPs of BCRP may also be involved in the intestinal toxicity of SN-38, an active metabolite of irinotecan. Since BCRP also transports SN-38 (28), it is possible that subjects who have Q141K or S441N SNPs variants of BCRP are more sensitive to SN-38.

In conclusion, we have shown that two kinds of SNP variants of BCRP (Q141K and S441N BCRP) are associated with the reduced expression. In particular, S441N variation is associated with the altered cellular localization. Since the allele frequency of Q141K in Japanese subjects is as high as 29-36%, it is possible that the interindividual variations in *in vivo* disposition of BCRP substrates may result from the genotype of BCRP.

ACKNOWLEDGMENTS

This work was supported by a grant-in-aid from the Ministry of Education, Science, Culture and Sports for the 21st Century Center of Excellence program and by Health and Labor Sciences Research Grants from the Ministry of Health, Labor, and Welfare for the Research on Advanced Medical Technology.

REFERENCES

1. L. A. Doyle, W. Yang, L. V. Abruzzo, T. Krogmann, Y. Gao, A. K. Rishi, and D. D. Ross. A multidrug resistance transporter from human MCF-7 breast cancer cells. *Proc. Natl. Acad. Sci. USA* **95**:15665–15670 (1998).
2. K. Miyake, T. Litman, R. Robey, and S. E. Bates. Reversal of resistance by GF120918 in cell lines expressing the ABC half-transporter, MXR. *Cancer Lett.* **146**:117–126 (1999).
3. R. Allikmets, L. M. Schriml, A. Hutchinson, V. Romano-Spica, and M. Dean. A human placenta-specific ATP-binding cassette gene (ABCP) on chromosome 4q22 that is involved in multidrug resistance. *Cancer Res.* **58**:5337–5339 (1998).
4. J. D. Allen, R. F. Brinkhuis, J. Wijnholds, and A. H. Schinkel. The mouse Bcrp1/Mxr/Abcp gene: amplification and overexpression in cell lines selected for resistance to topotecan, mitoxantrone, or doxorubicin. *Cancer Res.* **59**:4237–4241 (1999).
5. K. J. Bailey-Dell, B. Hassel, L. A. Doyle, and D. D. Ross. Promoter characterization and genomic organization of the human breast cancer resistance protein (ATP-binding cassette transporter G2) gene. *Biochim. Biophys. Acta* **1520**:234–241 (2001).
6. K. Kage, S. Tsukahara, T. Sugiyama, S. Asada, E. Ishikawa, T. Tsuruo, and Y. Sugimoto. Dominant-negative inhibition of breast cancer resistance protein as drug efflux pump through the inhibition of S-S dependent homodimerization. *Int. J. Cancer* **97**:626–630 (2002).
7. T. Litman, T. E. Druley, W. D. Stein, and S. E. Bates. From MDR to MXR: new understanding of multidrug resistance systems, their properties and clinical significance. *Cell. Mol. Life Sci.* **58**: 931–959 (2001).
8. M. Maliepaard, G. L. Scheffer, I. F. Faneyte, M. A. van Gastelen, A. C. Pijnenborg, A. H. Schinkel, M. J. van De Vijver, R. J. Scheper, and J. H. Schellens. Subcellular localization and distribution of the breast cancer resistance protein transporter in normal human tissues. *Cancer Res.* **61**:3458–3464 (2001).
9. J. W. Jonker, J. W. Smit, R. F. Brinkhuis, M. Maliepaard, J. H. Beijnen, J. H. Schellens, and A. H. Schinkel. Role of breast cancer resistance protein in the bioavailability and fetal penetration of topotecan. *J. Natl. Cancer Inst.* **92**:1651–1656 (2000).
10. J. W. Jonker, M. Buitelaar, E. Wagenaar, M. A. van der Valk, G. L. Scheffer, R. J. Scheper, T. Plosch, F. Kuipers, R. P. Oude Elferink, H. Rosing, J. H. Beijnen, and A. H. Schinkel. The breast cancer resistance protein protects against a major chlorophyll-derived dietary phototoxin and protoporphyria. *Proc. Natl. Acad. Sci. USA* **99**:15649–15654 (2002).
11. M. Suzuki, H. Suzuki, Y. Sugimoto, and Y. Sugiyama. ABCG2 transports sulfated conjugates of steroids and xenobiotics. *J. Biol. Chem.* **278**:22644–22649 (2003).
12. Y. Honjo, C. A. Hrycyna, Q. W. Yan, W. Y. Medina-Perez, R. W. Robey, A. van de Laar, T. Litman, M. Dean, and S. E. Bates. Acquired mutations in the MXR/BCRP/ABCP gene alter substrate specificity in MXR/BCRP/ABCP-overexpressing cells. *Cancer Res.* **61**:6635–6639 (2001).
13. H. Mitomo, R. Kato, A. Ito, S. Kasamatsu, Y. Ikegami, I. Kii, A. Kudo, E. Kobatake, Y. Sumino, and T. Ishikawa. A functional study on polymorphism of the ATP-binding cassette transporter ABCG2: critical role of arginine-482 in methotrexate transport. *Biochem. J.* **373**:767–774 (2003).
14. M. Itoda, Y. Saito, K. Shirao, H. Minami, A. Ohtsu, T. Yoshida, N. Saijo, H. Suzuki, Y. Sugiyama, S. Ozawa, and J.-I. Sawada. Eight novel single nucleotide polymorphisms in *ABCG2/BCRP* in Japanese cancer patients administered irinotecan. *Drug Metab. Pharmacokinet.* **18**:212–217 (2003).
15. H. Mizuguchi and M. A. Kay. Efficient construction of a recom-

binant adenovirus vector by an improved in vitro ligation method. *Hum. Gene Ther.* 9:2577–2583 (1998).
16. H. Mizuguchi and M. A. Kay. A simple method for constructing E1- and E1/E4-deleted recombinant adenoviral vectors. *Hum. Gene Ther.* **10**:2013–2017 (1999).
17. M. Muller, C. Meijer, G. J. Zaman, P. Borst, R. J. Scheper, N. H. Mulder, E. G. de Vries, and P. L. Jansen. Overexpression of the gene encoding the multidrug resistance-associated protein results in increased ATP-dependent glutathione S-conjugate transport. *Proc. Natl. Acad. Sci. USA* **91**:13033–13037 (1994).
18. T. Hirohashi, H. Suzuki, X. Y. Chu, I. Tamai, A. Tsuji, and Y. Sugiyama. Function and expression of multidrug resistance-associated protein family in human colon adenocarcinoma cells (Caco-2). *J. Pharmacol. Exp. Ther.* **292**:265–270 (2000).
19. Y. Imai, M. Nakane, K. Kage, S. Tsukahara, E. Ishikawa, T. Tsuruo, Y. Miki, and Y. Sugimoto. C421A polymorphism in the human breast cancer resistance protein gene is associated with low expression of Q141K protein and low-level drug resistance. *Mol. Cancer Ther.* **1**:611–616 (2002).
20. C. P. Zamber, J. K. Lamba, K. Yasuda, J. Farnum, K. Thummel, J. D. Schuetz, and E. G. Schuetz. Natural allelic variants of breast cancer resistance protein (BCRP) and their relationship to BCRP expression in human intestine. *Pharmacogenetics* **13**:19–28 (2003).
21. G. Backstrom, J. Taipalensuu, H. Melhus, H. Brandstrom, A. C. Svensson, P. Artursson, and A. Kindmark. Genetic variation in the ATP-binding Cassette Transporter gene ABCG2 (BCRP) in a Swedish population. *Eur. J. Pharm. Sci.* **18**:359–364 (2003).
22. K. Hashimoto, T. Uchiumi, T. Konno, T. Ebihara, T. Nakamura, M. Wada, S. Sakisaka, F. Maniwa, T. Amachi, K. Ueda, and M. Kuwano. Trafficking and functional defects by mutations of the ATP-binding domains in MRP2 in patients with Dubin-Johnson syndrome. *Hepatology* **36**:1236–1245 (2002).
23. S. Mizuarai, N. Aozasa, and H. Kotani. Single nucleotide polymorphisms result in impaired membrane localization and reduced ATPase activity in multidrug transporter ABCG2. *Int. J. Cancer* **109**:238–246 (2004).
24. E. L. Volk and E. Schneider. Wild-type breast cancer resistance protein (BCRP/ABCG2) is a methorexate polyglutamate transporter. *Cancer Res.* **63**:5538–5543 (2003).
25. Z. S. Chen, R. W. Robey, M. G. Belinsky, I. Shchaveleva, X. Q. Ren, Y. Sugimoto, D. D. Ross, S. E. Bates, and G. D. Kruh. Transport of methotrexate, methotrexate polyglutamates, and 17β estraciol 17β-D-glucuronide by ABCG2: effects of acquired mutations at R482 on methotrexate transport. *Cancer Res.* **64**: 4048–4054 (2003).
26. S. Zhou, J. J. Morris, Y. Barnes, L. Lan, J. D. Schuetz, and B. P. Sorrentino. Bcrp1 gene expression is required for normal numbers of side population stem cells in mice, and confers relative protection to mitoxantrone in hematopoietic cells in vivo. *Proc. Natl. Acad. Sci. USA* **99**:12339–12344 (2002).
27. J. Taipalensuu, H. Tornblom, G. Lindberg, C. Einarsson, F. Sjoqvist, H. Melhus, P. Garberg, B. Sjostrom, B. Lundgren, and P. Artursson. Correlation of gene expression of ten drug efflux proteins of the ATP-binding cassette transporter family in normal human jejunum and in human intestinal epithelial Caco-2 cell monolayers. *J. Pharmacol. Exp. Ther.* **299**:164–170 (2001).
28. K. Nakatomi, M. Yoshikawa, M. Oka, Y. Ikegami, S. Hayasaka, K. Sano, K. Shiozawa, S. Kawabata, H. Soda, T. Ishikawa, S. Tanabe, and S. Kohno. Transport of 7-ethyl-10-hydroxy-camptothecin (SN-38) by breast cancer resistance protein ABCG2 in human lung cancer cells. *Biochem. Biophys. Res. Commun.* **288**:827–832 (2001).

0022-3565/04/3111-228–236$20.00
THE JOURNAL OF PHARMACOLOGY AND EXPERIMENTAL THERAPEUTICS
Copyright © 2004 by The American Society for Pharmacology and Experimental Therapeutics
JPET 311:228–236, 2004

Vol. 311, No. 1
68536/1171497
Printed in U.S.A.

Gemfibrozil and Its Glucuronide Inhibit the Organic Anion Transporting Polypeptide 2 (OATP2/OATP1B1:*SLC21A6*)-Mediated Hepatic Uptake and CYP2C8-Mediated Metabolism of Cerivastatin: Analysis of the Mechanism of the Clinically Relevant Drug-Drug Interaction between Cerivastatin and Gemfibrozil

Yoshihisa Shitara, Masaru Hirano, Hitoshi Sato, and Yuichi Sugiyama

School of Pharmaceutical Sciences, Showa University, Tokyo, Japan (Y.Sh., H.S.); and Graduate School of Pharmaceutical Sciences, The University of Tokyo, Tokyo, Japan (M.H., Y.Su.)

Received March 16, 2004; accepted June 10, 2004

ABSTRACT

A serious pharmacokinetic interaction between cerivastatin (CER) and gemfibrozil (GEM) has been reported. In the present study, we examined the inhibitory effects of GEM and its metabolites, M3 and gemfibrozil 1-*O*-β-glucuronide (GEM-1-*O*-glu), on the uptake of CER by human organic anion transporting polypeptide 2 (OATP2)-expressing cells and its metabolism in cytochrome P450 expression systems. Uptake studies showed that GEM and GEM-1-*O*-glu significantly inhibited the OATP2-mediated uptake of CER with IC_{50} values of 72 and 24 μM, respectively. They also inhibited the CYP2C8-mediated metabolism of CER with IC_{50} values of 28 and 4 μM, respectively, whereas M3 had no effects. GEM and GEM-1-*O*-glu minimally inhibited the CYP3A4-mediated metabolism of CER. The IC_{50} values of GEM and GEM-1-*O*-glu for the uptake and the metabolism of CER obtained in the present study were lower than their total, and not unbound, plasma concentrations. However, considering the possibly concentrated high unbound concentrations of GEM-1-*O*-glu in the liver and its relatively larger plasma unbound fraction compared with GEM itself, the glucuronide inhibition of the CYP2C8-mediated metabolism of CER appears to be the main mechanism for the clinically relevant drug-drug interaction. Previously reported clinical drug interaction studies showing that coadministration of GEM with pravastatin or pitavastatin, both of which are known to be cleared from the plasma by the uptake transporters in the liver, only minimally (less than 2-fold) increased the area under the plasma concentration-time curve of these statins, also supported our present conclusion.

3-Hydroxy-3-methylglutaryl CoA reductase inhibitors (statins) and fibrates are now well established treatments for hyperlipidemia to prevent cardiovascular diseases (Wierzbicki et al., 2003). Statins are principally used to reduce low density lipoprotein and also triglycerides in proportion to their low density lipoprotein-lowering efficacy and the baseline triglyceride level, whereas fibrates are mainly used for the treatment of hypertriglyceridemia or as second-line agents in patients with statin intolerance (Moghadasian et al., 2000; Wierzbicki et al., 2003). The combination therapy of statins and fibrates is widely used in clinical practice; however, there are reports of rhabdomyolysis by this combination therapy, mainly involving gemfibrozil (GEM) with lovastatin and cerivastatin (CER) (Abdul-Ghaffar and El-Sonbaty, 1995; Bruno-Joyce et al., 2001; Roca et al., 2002). This may be partly due to drug-drug interactions (DDI) caused by events at a pharmacokinetic level, although an event at a pharmacodynamic

This study was supported in part by a grant-in-aid for Young Scientists (B) provided by the Ministry of Education, Culture, Sports, Science and Technology, Japan (Y.Sh.), a grant-in-aid for the Advanced and Innovational Research Program in Life Sciences from the Ministry of Education, Culture, Sports, Science and Technology, Japan (Y.Su.), and a Health and Labor Sciences Research grant from the Ministry of Health, Labor and Welfare, Japan, for the Research on Advanced Medical Technology (Y.Su.).
Article, publication date, and citation information can be found at http://jpet.aspetjournals.org.
doi:10.1124/jpet.104.068536.

ABBREVIATIONS: GEM, gemfibrozil; CER, cerivastatin; DDI, drug-drug interaction; AUC, area under the plasma concentration-time curve; P450, cytochrome P450; UGT, uridine diphosphate glucuronosyltransferase; K_i, inhibition constant; GEM-1-*O*-glu, gemfibrozil 1-*O*-β-glucuronide; HPLC, high-performance liquid chromatography; IC_{50}, concentration of inhibitor to produce a 50% reduction in the metabolism or transport; HLM, human liver microsome; Ab, antibody; TLC, thin-layer chromatography; CL_{uptake}, uptake clearance.

level, i.e., a strong direct effect on myocytes by combination therapy, may be also involved (Kyrklund et al., 2001; Backman et al., 2002; Matzno et al., 2003). Indeed, concomitant use of GEM markedly increased the area under the plasma concentration-time curve (AUC) of simvastatin acid, lovastatin acid, and CER and produced a small increase in the concentrations of pravastatin and pitavastatin (Backman et al., 2000, 2002; Kyrklund et al., 2001, 2003; Mathew et al., 2004). Staffa et al. (2002) reported that 31 patients taking CER died due to rhabdomyolysis, and 12 of them were concomitantly taking GEM. Due to this severe side effect, CER was voluntarily withdrawn from the world market in August 2001.

Reports have appeared describing the mechanism of the pharmacokinetic interaction between CER and GEM (Wen et al., 2001; Prueksaritanont et al., 2002b,c; Wang et al., 2002). In humans, CER is subject to a dual metabolic pathway mediated by CYP2C8 and CYP3A4 (Mück, 2000). Wen et al. (2001) and Wang et al. (2002) reported that GEM inhibits multiple isoforms of cytochromes P450 (P450s), including CYP2C8, but has no inhibitory effect on CYP3A4. Therefore, the inhibition of CYP2C8-mediated metabolism may be one mechanism responsible for this clinically relevant DDI. In addition, Prueksaritanont et al. (2002a) have suggested that UGT-mediated glucuronidation of statins is an important metabolic pathway because they are spontaneously converted to lactones following UGT-mediated glucuronidation. Prueksaritanont et al. (2002b,c) have also reported that GEM inhibits this UGT-mediated glucuronidation of CER as well as P450-mediated oxidation. The inhibition constants (K_i) or the concentrations of inhibitors to produce a 50% reduction in the metabolism of CER (IC_{50}) in their reports were as high as the total plasma concentration of GEM in the therapeutic range (Prueksaritanont et al., 2002b,c; Wang et al., 2002); however, taking the high protein binding of GEM into consideration, the unbound concentration of GEM is much less than the reported K_i or IC_{50} values (Todd and Ward, 1988; Prueksaritanont et al., 2002c; Wang et al., 2002).

We previously reported that CER was actively taken up into the liver via transporter(s) including organic anion transporting polypeptide 2 [OATP2 (OATP1B1); *SLC21A6*] (Shitara et al., 2003). We investigated the inhibitory effects of cyclosporin A on the transporter-mediated uptake of CER in hepatocytes and showed that cyclosporin A inhibited it without any effects on its metabolism at therapeutic concentrations (Shitara et al., 2003). This partly explained the mechanism responsible for the clinically relevant DDI between CER and cyclosporin A (Shitara et al., 2003); however, there have been no reports of the interaction between GEM and transporters until now. Gemfibrozil 1-*O*-β-glucuronide (GEM-1-*O*-glu), a metabolite of GEM, is taken up and accumulates in isolated perfused rat liver (Sallustio et al., 1996; Sabordo et al., 1999, 2000). This uptake is inhibited by coadministration of dibromosulfophthalein and clofibric acid, whereas acetaminophen and its glucuronide produced no inhibition (Sabordo et al., 1999, 2000). These results suggest an involvement of transporter(s) in the hepatic uptake of GEM-1-*O*-glu, and therefore, GEM-1-*O*-glu may affect the transporter-mediated uptake of CER.

GEM is metabolized to M1–4 by P450s with M3 being the major metabolite (Nakagawa et al., 1991). GEM also undergoes glucuronidation, mainly to GEM-1-*O*-glu (Nakagawa et al., 1991), and the plasma concentrations of these metabolites are reported to be relatively high (Okerholm et al., 1976; Nakagawa et al., 1991). Therefore, in the present study, we examined the effects of GEM and its major metabolites, M3 and GEM-1-*O*-glu, on the metabolism and the transporter-mediated uptake of CER to analyze the mechanism of the clinically relevant DDI between CER and GEM.

Materials and Methods

Materials. [^{14}C]CER (2.03 GBq/mmol) and unlabeled CER were kindly provided by Bayer AG (Wuppertal, Germany). GEM was purchased from Sigma-Aldrich (St. Louis, MO). A metabolite of GEM, M3 (purity: 99.6%), was chemically synthesized in KNC Laboratories, Co. Ltd. (Kobe, Japan). GEM-1-*O*-glu was enzymatically synthesized from GEM. GEM (2 mg/ml) was incubated at 37°C with rat microsomes (3.6 mg of protein/ml) and 5 mg/ml UDP glucuronic acid in 100 mM glycine-NaOH buffer (pH 8.5) supplemented with 20% (w/v) glycerin for 27 h, followed by the addition of 1 N HCl to bring the pH to 4.0. This sample was chromatographed on an ODS column (Cosmosil 75C_{18}-PREP, 300 ml; Nakalai Tesque, Kyoto, Japan) with MeOH/H_2O (30:70–80:20, stepwise) as the mobile phase and analyzed by high-performance liquid chromatography (HPLC) using an ODS column (Inertsil ODS-2, φ4.6 × 150 mm; GL Sciences, Inc., Tokyo, Japan) with a mobile phase of 0.05% trifluoroacetic acid/acetonitrile (53:47) at a flow rate of 1.0 ml/min. The fraction containing GEM-1-*O*-glu, detected by its absorbance at 254 nm, was collected and evaporated. The fraction was rechromatographed on an ODS column with MeOH/H_2O (50:50–80:20, stepwise) and purified, followed by evaporation, to obtain GEM-1-*O*-glu. The purity was 99.4% determined by HPLC detected by the absorbance at 230 nm. The chemical structures and molecular weights of M3 and GEM-1-*O*-glu were confirmed by NMR and mass spectrometry (MS) analyses, respectively. The chemical structures of GEM and its metabolites used in the present study are shown in Fig. 1. All other reagents were of analytical grade.

Uptake of [^{14}C]CER in OATP2-Expressing Cells. An uptake study of CER in OATP2-expressing cells was conducted in the presence of GEM and its metabolites, M3 and GEM-1-*O*-glu. The construction of OATP2-expressing Madin-Darby canine kidney (MDCK) cells has been previously described (Sasaki et al., 2002). The uptake of [^{14}C]CER was examined by the method described previously (Shitara et al., 2003). The inhibitors, GEM (0–300 μM), M3 (0–1000 μM), or GEM-1-*O*-glu (0–300 μM), were added along with [^{14}C]CER when the uptake reaction was initiated.

In Vitro Metabolism of CER. To measure the effect of GEM and its metabolites on the metabolism of [^{14}C]CER and to estimate the contributions of CYP2C8 and 3A4, its in vitro metabolism was examined in CYP2C8- and 3A4-expressing insect cells supplemented with the expression of human P450 reductase and cytochrome b_5 (Supersome; BD Gentest, Woburn, MA) and pooled human liver microsomes (HLM; BD Gentest). To estimate the contribution of CYP2C8, HLM was preincubated with a specific inhibitory antibody (Ab) against CYP2C8 (BD Gentest; 0–10 μl/0.1 mg protein HLM) at 4°C for 20 min. To estimate the contribution of CYP3A4, ketoconazole (0–1 μM), a potent CYP3A4 inhibitor, was used. Prior to the metabolism study, human CYP2C8 and 3A4 expression systems (final 20 nM P450) or HLM (final 0.2 mg of protein/ml) were incubated at 37°C for 10 min in 100 mM potassium phosphate buffer (pH 7.4) containing 3.3 mM $MgCl_2$, 3.3 mM glucose 6-phosphate, 0.4 U/ml glucose-6-phosphate dehydrogenase, 1.3 mM NADPH, and 0.8 mM NADH. A 500-μl volume of incubation mixture was transferred to a polyethylene tube, and [^{14}C]CER (0.25 μM) was added to initiate the reaction with GEM, M3, or GEM-1-*O*-glu (0–300 μM). After incubation for 30 min, the reaction was terminated by the addition of 500 μl of ice-cold acetonitrile because this method had been shown to terminate the enzymatic reaction in a pilot study (data not shown),

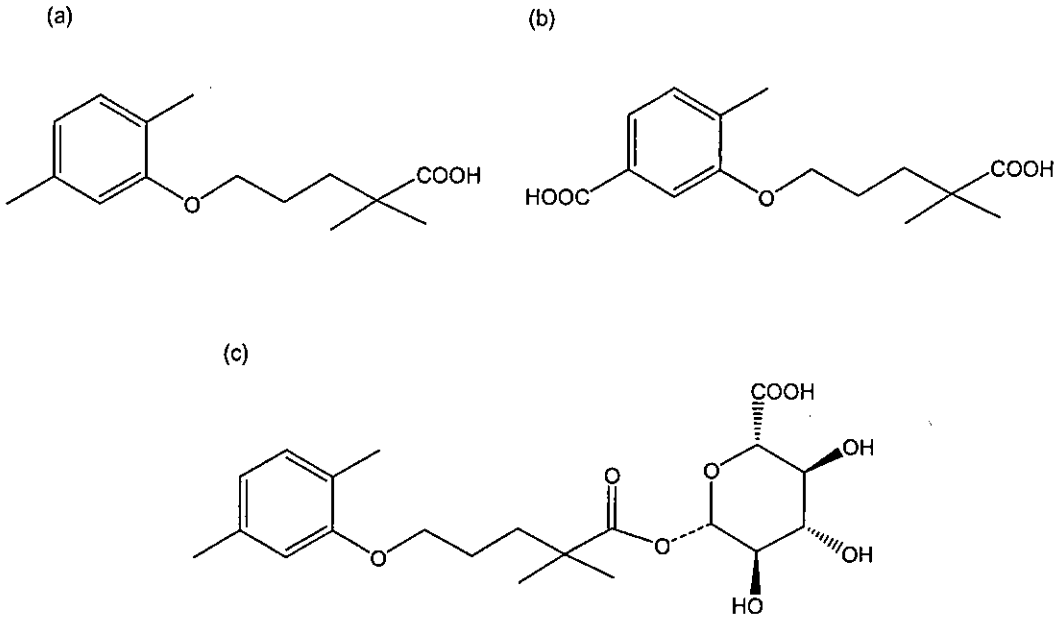

Fig. 1. Chemical structures of GEM and its metabolites. a, GEM; b, M3; c, GEM-1-*O*-glu.

subsequently followed by centrifugation. To measure the metabolic rate of [^{14}C]CER, the supernatant was collected and concentrated to approximately 20 μl in a centrifugal concentrator (VC-36N; TAITEC, Saitama, Japan), followed by thin-layer chromatography (TLC). The analyte was separated on silica gel 60F_{254} (Merck KGaA, Darmstadt, Germany) using a suitable mobile phase (toluene/acetone/acetic acid, 70:30:5, v/v). The intensity of the bands for intact [^{14}C]CER and its metabolites separated by TLC was determined by the BAS 2000 system (Fuji Film, Tokyo, Japan).

Protein Binding of GEM and Its Metabolites. To estimate the fraction not bound to human serum protein, 300 μM GEM, M3, and GEM-1-*O*-glu were added to serum (Nissui Pharmaceuticals, Inc., Tokyo, Japan), buffered with 50 mM potassium phosphate at 37°C, and incubated for 2 min. After that, the sample underwent ultrafiltration (Amicon Centrifree; Millipore Corporation, Billerica, MA) and the GEM and its metabolites in the filtrate were determined by HPLC. Phosphate-buffered saline (0.5 ml) containing 5 μl of 1 mM ibuprofen (internal standard) and 20 μl of formic acid were added to 0.5 ml of filtrate, followed by vigorous shaking. Subsequently, the sample was extracted with 5 ml of ethyl acetate/cyclohexane (20:80); then 4 ml of the organic phase was collected and evaporated. The sample obtained was dissolved in 0.5 ml of acetonitrile and separated on an ODS column (Super ODS column, ϕ4.6 × 150 mm; Tosoh, Tokyo, Japan). The mobile phase for GEM was 10 mM acetate buffer (pH 4.7)/acetonitrile (55:45), whereas that for M3 and GEM-1-*O*-glu was a mixture of 10 mM acetate buffer (pH 4.7) and acetonitrile with a linear gradient from 70 to 55% acetate buffer for 30 min, and the flow rate was 1.0 ml/min for all analyses. The retention times for GEM and ibuprofen were 28 and 13 min, respectively, and those for M3, GEM-1-*O*-glu, and ibuprofen were 13.5, 10, and 31 min, respectively. The absorbance was measured at 254 nm, and quantitation was carried out by comparison with the absorbance of a standard curve prepared for each compound.

Data Analysis. The time courses of the uptake of [^{14}C]CER into OATP2-expressing cells were expressed as the uptake volume (μl/mg protein) of radioactivity taken up into the cells (dpm/mg protein) divided by the concentration of radioactivity in the incubation buffer (dpm/μl). The uptake velocity of [^{14}C]CER was calculated using the uptake volume obtained at 2 min and expressed as the uptake clearance (CL_{uptake}: μl/min/mg protein). The metabolic rate of [^{14}C]CER was calculated by the decrease in unchanged [^{14}C]CER or the formation of its metabolites, M1 and M23.

To calculate the IC_{50} values of GEM and its metabolites in terms of the OATP2-mediated uptake, the following equation was used:

$$\Delta CL_{uptake}(+\text{inhibitor}) = \frac{\Delta CL_{uptake}(\text{control})}{1 + I/IC_{50}} \quad (1)$$

where ΔCL_{uptake} is the CL_{uptake} for OATP2-mediated uptake, which is the CL_{uptake} of [^{14}C]CER minus that estimated in the presence of excess unlabeled CER, ΔCL_{uptake}(+inhibitor) and ΔCL_{uptake}(control) are the ΔCL_{uptake} values estimated in the presence and absence of inhibitors, respectively, and I is the inhibitor concentrations.

For the inhibitory effects of GEM and its metabolites on the metabolism of [^{14}C]CER in CYP2C8 and 3A4 expression systems, the IC_{50} values were calculated from the following equation:

$$v(+\text{inhibitor}) = \frac{v(\text{control})}{1 + I/IC_{50}} \quad (2)$$

where v(+inhibitor) and v(control) are the metabolic rates of CER in the presence and absence of inhibitors, respectively.

These equations were fitted to the data obtained in the present study using a computerized version of the nonlinear least-squares method, WinNonlin (Pharsight, Mountain View, CA) to obtain the IC_{50} values with computer-calculated S.D. values.

For the inhibition study using pooled HLM, the observed values of the metabolic rates were compared with the simulated values using the following equation:

$$v(+\text{inhibitor}) = v(\text{control}) \times \left(\frac{R_{CYP2C8}}{1 + I/IC_{50\_2C8}} + \frac{R_{CYP3A4}}{1 + I/IC_{50\_3A4}} \right) \quad (3)$$

where, R_{CYP2C8} and R_{CYP3A4} are the contributions of CYP2C8 and 3A4 to the metabolism of CER (total metabolism and the formations of M1 and M23), respectively, and IC_{50_2C8} and IC_{50_3A4} are the IC_{50} values for CYP2C8- and 3A4-mediated metabolism of CER, respectively. For this simulation, the contributions of CYP2C8 and 3A4 to the formation of M1 and M23 in HLM were calculated based on the contributions of these enzymes to the total metabolism of CER in HLM and the ratio of the initial formation rate of each metabolite in P450 expression systems to that in HLM.

Results

Inhibitory Effects of GEM and Its Metabolites on OATP2-Mediated Uptake of [^{14}C]CER. The effects of GEM, M3, and its glucuronide on the OATP2-mediated uptake of [^{14}C]CER were examined (Fig. 2). GEM and GEM-1-*O*-glu significantly inhibited OATP2-mediated uptake of [^{14}C]CER without any effects on the uptake in vector-transfected cells, whereas M3 did not show a statistically significant inhibition up to a concentration of 1000 μM (Fig. 2). The IC_{50} values of GEM and GEM-1-*O*-glu for the OATP2-mediated uptake of [^{14}C]CER were 72.4 ± 28.4 and 24.3 ± 19.8 μM, respectively (mean ± S.D.).

Inhibitory Effects of GEM and its Metabolites on the in Vitro Metabolism of [^{14}C]CER in CYP2C8 and 3A4 Expression Systems. The in vitro metabolism of [^{14}C]CER was examined in CYP2C8 and 3A4 expression systems. In the TLC analysis, one band for parent [^{14}C]CER and two other bands for metabolites were detected in the CYP2C8 expression system, whereas one band for [^{14}C]CER and only one band for a metabolite were detected in the CYP3A4 expression system. The band for one of the metabolites produced by CYP2C8 and CYP3A4 matched, suggesting that these two enzymes produced the same metabolite. This metabolite was identified as M1 and the other was M23. The Rf values for [^{14}C]CER, M1, and M23 were 0.13, 0.09, and 0.055, respectively. In Fig. 3, the metabolism of [^{14}C]CER in the CYP2C8 and 3A4 expression systems in the presence or absence of GEM and its metabolites are shown. GEM and GEM-1-*O*-glu significantly inhibited the metabolism of [^{14}C]CER in CYP2C8 and 3A4 expression systems, whereas M3 had no effects (Fig. 3). GEM and GEM-1-*O*-glu preferentially inhibited CYP2C8-mediated metabolism compared with CYP3A4-mediated metabolism (Fig. 3). The IC_{50} values of GEM and GEM-1-*O*-glu for the CYP2C8-mediated metabolism were 28.0 ± 4.3 and 4.07 ± 1.23 μM (mean ± S.D.), respectively, and the corresponding values for the CYP3A4-mediated metabolism were 372 ± 100 and 243 ± 59 μM (mean ± S.D.), respectively. In Figs. 4 and 5, the CYP2C8-mediated M1 and M23 formation rates and the CYP3A4-mediated M1 formation rate in the presence or absence of GEM and GEM-1-*O*-glu are shown. GEM and GEM-1-*O*-glu inhibited CYP2C8-mediated M1 formation with IC_{50} values of 36.8 ± 5.3 and 5.38 ± 1.29 μM (mean ± S.D.), respectively, and M23 formation with IC_{50} values of 29.7 ± 4.4 and 4.30 ± 1.48 μM (mean ± S.D.), respectively (Fig. 4). They slightly inhibited CYP3A4-mediated M1 formation with IC_{50} values of 406 ± 106 and 267 ± 62 μM (mean ± S.D.), respectively (Fig. 5). The IC_{50} values of GEM and GEM-1-*O*-glu for the OATP2-mediated uptake and the CYP2C8- and 3A4-mediated metabolism of [^{14}C]CER are summarized in Table 1.

Estimation of the Contributions of CYP2C8 and 3A4 to the Metabolism of [^{14}C]CER in Pooled HLM. To estimate the contributions of CYP2C8 and 3A4, we examined the effect of a specific inhibitory Ab for CYP2C8 and ketoconazole, a potent inhibitor of CYP3A4, on the metabolism of [^{14}C]CER in the pooled HLM (Fig. 6). Incubation with HLM produced three different metabolites detected by TLC, and one of them (Rf = 0.04) was identified as M24, a metabolite spontaneously produced from M1 and M23. In the present analysis, only the formation of M1 and M23 was analyzed. The inhibitory Ab for CYP2C8 inhibited the microsomal metabolism of [^{14}C]CER in a concentration-dependent manner at low concentrations, and maximum inhibition was obtained at 5 μl/100 μg of microsomes (Fig. 6a). At maximum inhibition, the microsomal metabolism of [^{14}C]CER decreased to 38.9 ± 2.7% (mean ± S.E.) of the control (Fig. 6a), and therefore, the contribution of CYP2C8 was estimated to be 61%. In the presence of inhibitory Ab for CYP2C8, M23 formation was completely inhibited, whereas M1 formation fell only to 61.2 ± 2.9% (mean ± S.E.) of the control (Fig. 6, b and c). Ketoconazole also reduced the microsomal metabolism of [^{14}C]CER in a concentration-dependent manner (Fig. 6d). However, the inhibition studies using CYP2C8 and 3A4 expression systems showed that it inhibited not only CYP3A4-mediated metabolism but also that mediated by CYP2C8 (Fig. 6d). At 0.1 μM, most of the CYP3A4-mediated metabolism of [^{14}C]CER was inhibited with only a minimal effect on that mediated by CYP2C8 (Fig. 6d); therefore, 0.1 μM ketoconazole was used to estimate the contribution of CYP3A4. It was found that 0.1 μM ketoconazole reduced the metabolism of [^{14}C]CER to 63.4 ± 7.2% (mean ± S.E.) of the control (Fig. 6d), suggesting that the contribution of CYP3A4

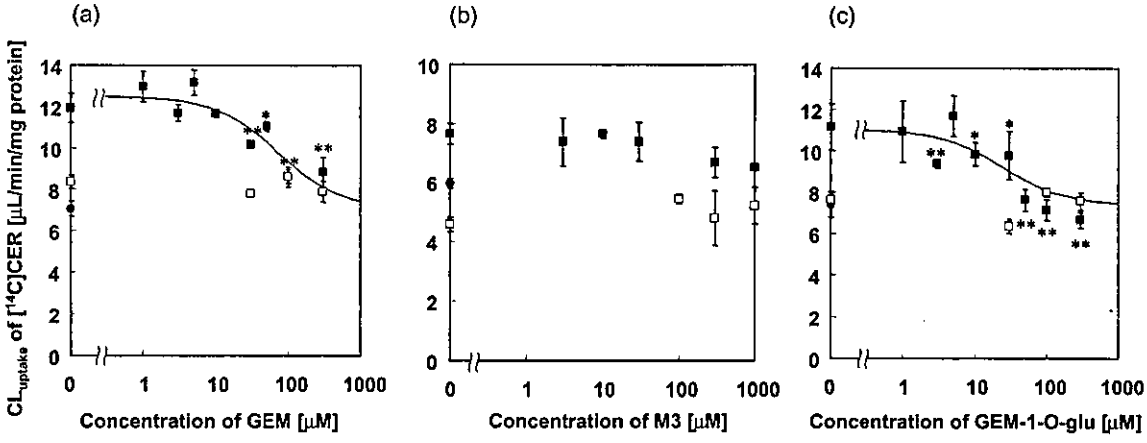

Fig. 2. Effect of GEM and its metabolites on the OATP2-mediated uptake of [^{14}C]CER. The inhibitory effects of GEM (a), M3 (b), and GEM-1-*O*-glu (c) on the OATP2-mediated uptake of [^{14}C]CER were examined. Uptake of [^{14}C]CER in OATP2-expressing (■) and vector-transfected (□) cells in the presence of GEM and its metabolites is shown. Uptake of [^{14}C]CER in the presence of excess unlabeled CER (30 μM) was also examined (●). Each symbol represents the mean value of three independent experiments ± S.E., and solid lines represent the fitted lines. The asterisks represent a statistically significant difference shown by Dunnett's test (*, $p < 0.05$; **, $p < 0.01$).

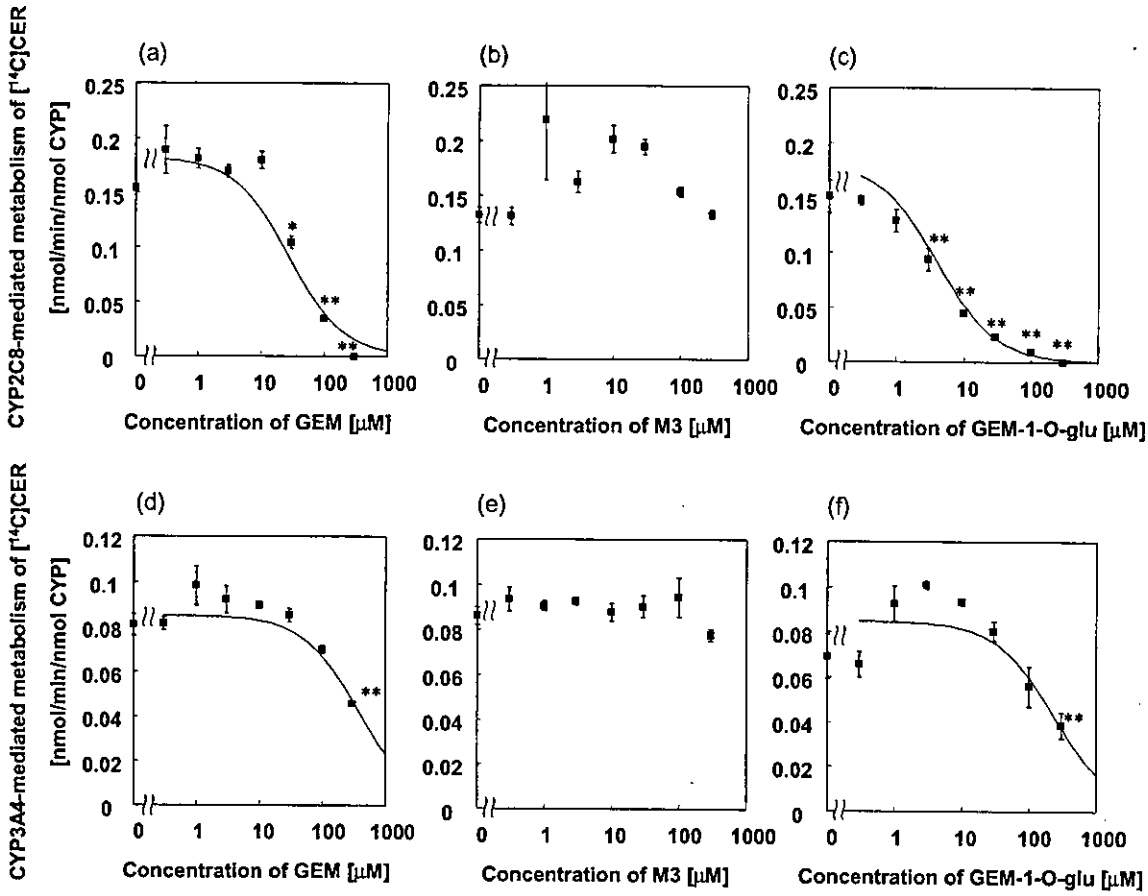

Fig. 3. Effect of GEM and its metabolites on the CYP2C8- and 3A4-mediated metabolism of [^{14}C]CER. Inhibitory effects of GEM (a, d), M3 (b, e), and GEM-1-*O*-glu (c, f) on the metabolism of [^{14}C]CER in CYP2C8 (a, b, c) and 3A4 (d, e, f) expression systems were examined. Each symbol represents the mean value of three independent experiments ± S.E., and solid lines represent the fitted lines. The asterisks represent a statistically significant difference by Dunnett's test (*, $p < 0.05$; **, $p < 0.01$).

was 37%, at most. In addition, 0.1 μM ketoconazole reduced M1 formation to 62.6 ± 5.6% (mean ± S.E.) of the control and slightly, but not significantly, reduced M23 formation to 77.6 ± 11.3% (mean ± S.E.) of the control (Fig. 6, e and f).

Inhibitory Effects of GEM and Its Metabolites on the in Vitro Metabolism of [^{14}C]CER in Pooled HLM. We examined the inhibitory effects of GEM and GEM-1-*O*-glu on the metabolism of [^{14}C]CER in pooled HLM (Fig. 7). GEM and GEM-1-*O*-glu inhibited the metabolism of [^{14}C]CER in pooled HLM in a concentration-dependent manner (Fig. 7), whereas M3 had no effects (data not shown). Figure 7 also shows simulation curves for the inhibitory effects of GEM and GEM-1-*O*-glu in pooled HLM based on eq. 3.

Human Serum Protein Binding of GEM and Its Metabolites. We examined the protein binding of GEM and its metabolites in 50 mM phosphate-buffered human serum (pH 7.4). The unbound fractions (f_u) of GEM, M3, and GEM-1-*O*-glu were 0.648 ± 0.037, 1.23 ± 0.00, 11.5 ± 2.3% (mean ± S.E.), respectively.

Discussion

It has already been reported that GEM is an inhibitor of P450- and UGT-mediated metabolism of CER (Prueksaritanont et al., 2002b,c; Wang et al., 2002). In the present study, we showed that GEM inhibited the OATP2-mediated uptake of CER as well as its metabolism (Fig. 2). The IC_{50} value of GEM for OATP2-mediated uptake of [^{14}C]CER (72 μM) was similar to, or lower than, the reported IC_{50} values for metabolism (Prueksaritanont et al., 2002b,c; Wang et al., 2002). We also found that a metabolite of GEM, GEM-1-*O*-glu, was a potent inhibitor of OATP2-mediated hepatic uptake of CER with a lower IC_{50} value (24 μM) than that of GEM itself (Fig. 2). This finding was matched by the fact that many glucuronides are recognized by OATP family transporters as substrates and/or inhibitors with a high affinity (König et al., 2000a,b, Cui et al., 2001).

We also examined the inhibitory effect of GEM and its metabolites on the CYP2C8- and 3A4-mediated metabolism of [^{14}C]CER. In the present TLC analysis, two clear bands for metabolites were detected in the experiment using the CYP2C8 expression system, whereas only one clear band for the metabolite was detected in the CYP3A4 experiment. Because Wang et al. (2002) reported that CYP2C8 and 3A4 equally catalyzed the formation of M1 although the formation rate of M23 was 14-fold lower in CYP3A4 than in CYP2C8, we identified these two bands as M1 and M23, respectively. The results of the inhibition studies should be discussed in relation to previous reports (Prueksaritanont et al., 2002c; Wang et al., 2002). Wang et al. (2002) reported that GEM inhibited CYP2C8-mediated metabolism of CER to M1 and M23 with IC_{50} values of 78 and 68 μM, respectively. The corresponding values in the present analysis were 37 and 30 μM, respectively (Fig. 4), and these are comparable

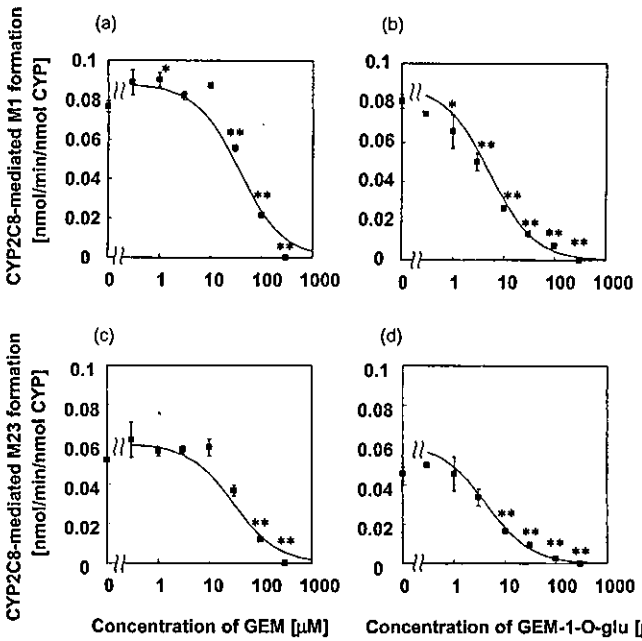

Fig. 4. Effect of GEM and GEM-1-*O*-glu on the CYP2C8-mediated M1 and M23 formation of [^{14}C]CER. Inhibitory effects of GEM (a, c) and GEM-1-*O*-glu (b, d) on the CYP2C8-mediated M1 formation (a, b) and M23 formation (c, d) were examined. Each symbol represents the mean value of three independent experiments ± S.E., and solid lines represent the fitted lines. The asterisks represent a statistically significant difference shown by Dunnett's test (*, $p < 0.05$; **, $p < 0.01$).

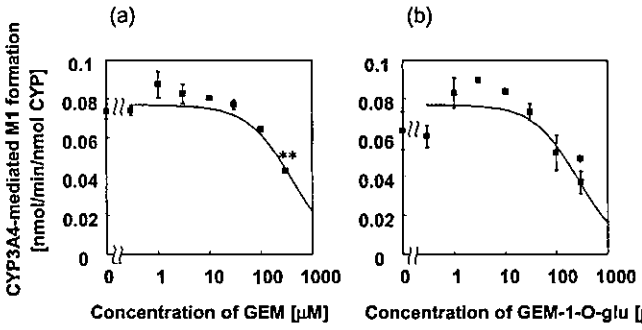

Fig. 5. Effect of GEM and GEM-1-*O*-glu on the CYP3A4-mediated M1 and M23 formation of [^{14}C]CER. Inhibitory effects of GEM (a) and GEM-1-*O*-glu (b) on the CYP3A4-mediated M1 formation were examined. Each symbol represents the mean value of three independent experiments ± S.E., and solid lines represent the fitted lines. The asterisks represent a statistically significant difference shown by Dunnett's test (*, $p < 0.05$; **, $p < 0.01$).

with the values reported by Wang et al. (2002). Prueksaritanont et al. (2002c) reported that the IC_{50} values of GEM for M1 and M23 formations in HLM were 220 and 87 μM, respectively, and Wang et al. (2002) reported the corresponding values to be >250 and 95 μM, respectively. As shown in Fig. 7, we also observed a concentration-dependent reduction in M1 and M23 formation in HLM. The apparent IC_{50} values of GEM for M1 and M23 formation in HLM was calculated to be 234 and 26 μM, respectively (Fig. 7), and these are also similar to results in previous reports (Prueksaritanont et al., 2002c; Wang et al., 2002).

Atypical effects of inhibitors were found in the present study, i.e., M3 apparently activated the CYP2C8-mediated metabolism of [^{14}C]CER at low concentrations, and GEM-1-*O*-glu activated the CYP3A4-mediated metabolism and M1

TABLE 1

IC_{50} values of GEM and GEM-1-*O*-glu on the OATP2-mediated uptake and metabolism of [^{14}C]CER[a]

	GEM	GEM-1-*O*-glu
	μM	
OATP2-mediated uptake	72.4 ± 28.4	24.3 ± 19.8
CYP2C8-mediated metabolism	28.0 ± 4.3	4.07 ± 1.23
CYP3A4-mediated metabolism	372 ± 100	243 ± 59

[a] All data are represented as the mean ± computer-calculated S.D.

formation at low concentrations, whereas it inhibited them at higher concentrations (Figs. 3 and 5), although these activations were not statistically significant with a few exceptions. These atypical effects of inhibitors may be explained by a multisite kinetic analysis involving a mixed effect of GEM and its metabolites as inhibitors and activators of enzymatic reactions (Galetin et al., 2002, 2003). However, in the present study, the enhancing effect was at most 1.5-fold, and this would have only a minimal effect on drug disposition in clinical situations, if any. Therefore, we analyzed the effects of GEM and its metabolites by a simple eq. 2.

In the present study, we showed that GEM and GEM-1-*O*-glu inhibited OATP2-mediated hepatic uptake and metabolism of [^{14}C]CER. Hence, the coadministration of GEM may lead to a DDI due to the inhibition of hepatic uptake and/or metabolism of CER. The possibility of a clinically relevant DDI should be discussed taking the therapeutic concentration of GEM and its metabolites into consideration because the intrinsic hepatic clearance will fall to $1/(1+ I/IC_{50})$ of control, where I is the inhibitor concentration (Ueda et al., 2001). In the report by Backman et al. (2002), the mean maximum concentration of GEM after repeated oral administration of 600 mg twice daily was 150 μM. Okerholm et al. (1976) measured the plasma concentrations of free GEM, its glucuronide conjugates, and other metabolites after a single oral administration of 600 mg of [^{3}H]GEM in normal human subjects receiving 600 mg of unlabeled GEM twice daily for 6 days and reported that the maximum concentration of glucuronide conjugates, mainly GEM-1-*O*-glu, was approximately 20 μM, whereas that of total GEM (GEM + glucuronide conjugate) was approximately 100 μM. Hengy and Kölle (1985) also reported that 10 to 15% of GEM in plasma was present as glucuronide conjugates. The reported values of the total concentrations of GEM and GEM-1-*O*-glu were similar or higher than the IC_{50} values for the metabolism and hepatic uptake of CER in the present study. However, because of the high plasma protein binding, the unbound concentrations of GEM and GEM-1-*O*-glu were at most 0.97 and 2.3 μM, respectively, i.e., less than the IC_{50} values obtained in the present study. Because only unbound drugs interact with transporters, this result suggests that it is unlikely to cause the reported serious DDI between CER and GEM. However, it is possible that GEM or its metabolites inhibit the metabolism of CER in the liver if they are actively transported to the liver and accumulate there. Indeed, Sallustio et al. (1996) have reported that GEM-1-*O*-glu is actively taken up by perfused rat liver and the liver/perfusate concentration ratio is 35 to 42. Assuming that it also accumulates in human liver, its unbound concentration there would be higher than the IC_{50} value for the microsomal metabolism, which gives a $1+ I/IC_{50}$ value of 3.1 to 3.2, i.e., more than a 3-fold reduction in the intrinsic hepatic clearance, suggesting that it may

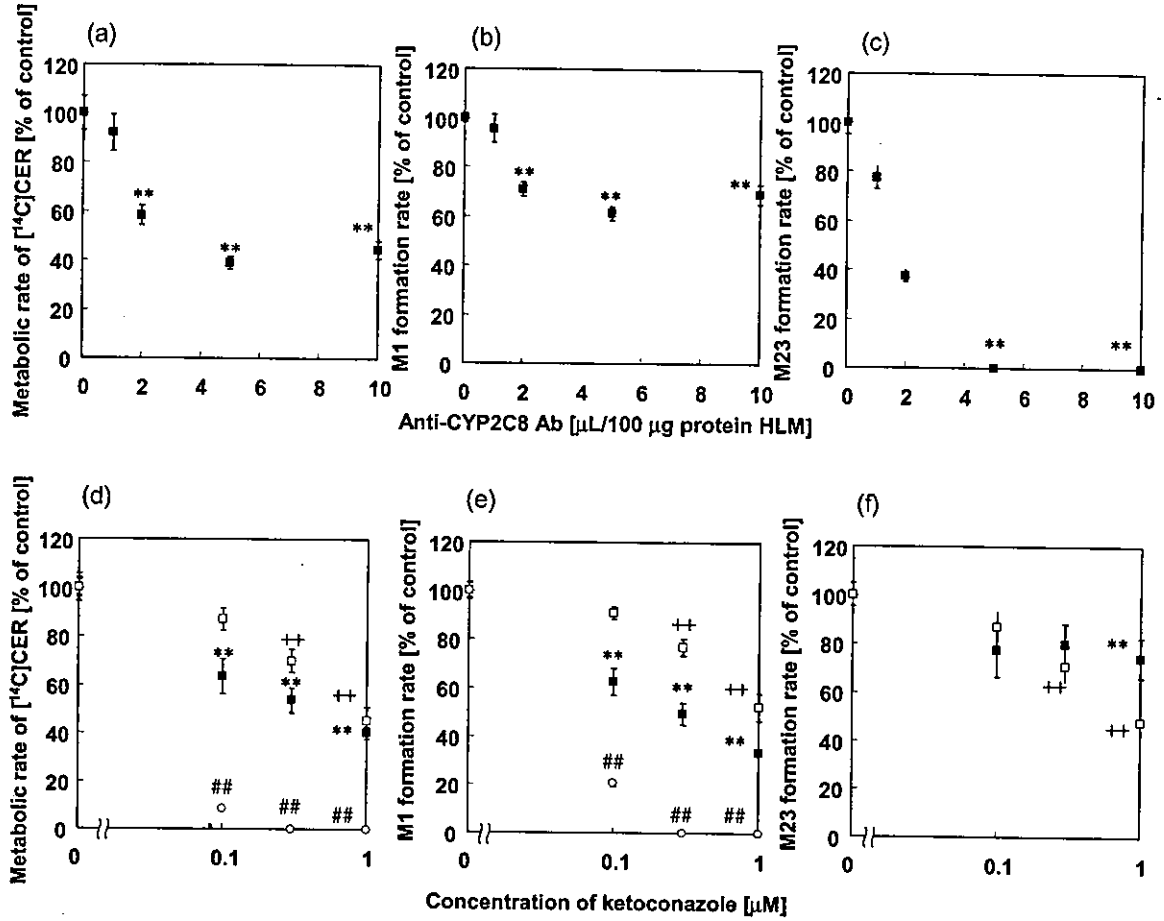

Fig. 6. Effect of specific inhibitory antibody against CYP2C8 (anti-CYP2C8 Ab) and ketoconazole on the metabolism of CER in HLM. The inhibitory effects of anti-CYP2C8 Ab (a) and ketoconazole, a potent CYP3A4 inhibitor (d), on the metabolism of [^{14}C]CER in pooled HLM (■) were examined. Their effects on M1 formation (b, e) and M23 formation (c, f) are also represented. The effect of ketoconazole on the metabolism of [^{14}C]CER in CYP2C8 (□) and CYP3A4 (○) expression systems was also examined. Each symbol represents the mean value of three independent experiments ± S.E., and solid lines represent the fitted lines. Symbols (*, +, and #) represent a statistically significant difference from the control values shown by Dunnett's test (*, $p < 0.05$; **, $p < 0.01$ for the metabolism in HLM; +, $p < 0.05$; ++, $p < 0.01$ for CYP2C8-mediated metabolism; and #, $p < 0.05$; ##, $p < 0.01$ for CYP3A4-mediated metabolism).

cause a serious DDI. In Table 2, the therapeutic total and unbound concentrations in the blood, the estimated unbound concentration in the liver, and the effects on the intrinsic hepatic clearances are summarized.

In the present study, GEM and GEM-1-*O*-glu preferentially inhibited CYP2C8-mediated metabolism of CER compared with CYP3A4-mediated metabolism (Figs. 3–5). These results support the findings by Backman et al. (2002) who reported that the AUC of M23 was markedly reduced to 17% of the control, whereas that of the open acid form of CER, the lactone form of CER, and M1 were 4.4, 3.5, and 3.5 times higher than the control. Because M23 formation is predominantly mediated by CYP2C8, and not by 3A4, the inhibition of CYP2C8 satisfactorily explains this DDI. In the report by Backman et al. (2002), all the AUC ratios for each of the metabolites to the open acid form of CER fell, following coadministration of GEM, to 82, 8.8, and 80% of the control for M1, M23, and the lactone form of CER, respectively. The slight reduction in the AUC of M1 and the lactone form may be partly due to GEM and GEM-1-*O*-glu inhibition of the hepatic uptake of CER, followed by M1 and M23 formation and lactonization in the liver.

Other statins, including simvastatin, lovastatin, pravastatin, and pitavastatin, are also affected by the coadministration of GEM (Backman et al., 2000, 2002; Kyrklund et al., 2001, 2003; Mathew et al., 2004). GEM increases the AUC of the open acid form of these statins (Backman et al., 2000, 2002; Kyrklund et al., 2001, 2003; Mathew et al., 2004). However, it does not affect the AUC of the lactone form of simvastatin and lovastatin and reduces that of pitavastatin (Backman et al., 2000; Kyrklund et al., 2001; Mathew et al., 2004), and it has no effect at all on the plasma concentration of fluvastatin (Spence et al., 1995). The limited effect of GEM only on the plasma concentrations of the open acid forms of simvastatin and lovastatin can be explained by inhibition of lactone formation followed by UGT-mediated glucuronidation (Prueksaritanont et al., 2002c). The reduced AUC of the lactone form of pitavastatin may also be explained by the same mechanism (Fujino et al., 2003). On the other hand, the increase in the AUC of the open acid forms of pravastatin and pitavastatin may be partly explained by minor inhibition of their OATP2-mediated uptake (Table 2), because these statins are substrates of OATP2 (Hsiang et al., 1999; Nakai et al., 2001; Hirano et al., 2004). GEM increases the AUC of pravastatin and pitavastatin only by 2.0- and 1.5-fold, respectively, whereas it increases that of CER 4.4-fold (Backman et al., 2002; Kyrklund et al., 2003; Mathew et al., 2004). The increase in the AUC of pravastatin can be partly ex-

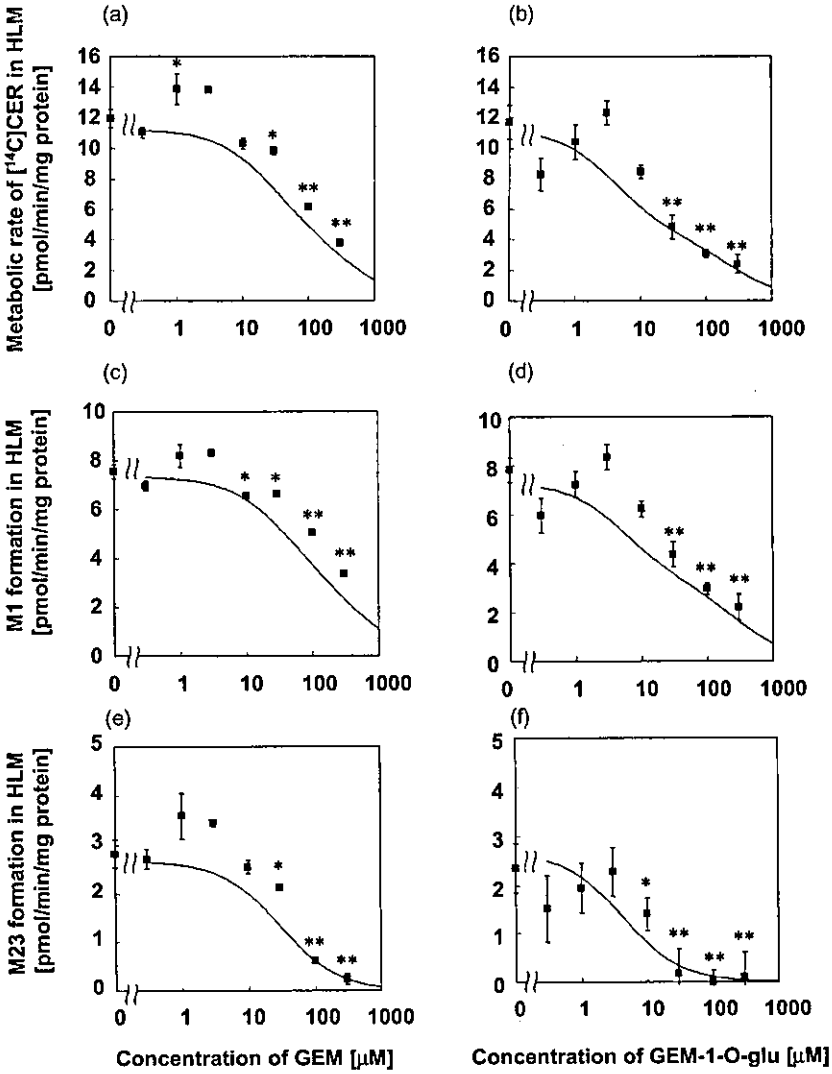

Fig. 7. Effect of GEM and its metabolites on the metabolism of [^{14}C]CER in HLM. The inhibitory effects of GEM (a, c, e) and GEM-1-*O*-glu (b, d, f) on the metabolism of [^{14}C]CER (a, b) and the formation of M1 (c, d) and M23 (e, f) in pooled HLM were examined. Each symbol represents the mean value of three independent experiments ± S.E. Solid lines represent simulated lines based on eq. 3. The asterisks represent a statistically significant difference shown by Dunnett's test (*, $p < 0.05$; **, $p < 0.01$).

TABLE 2
Plasma and liver concentrations of GEM and its metabolites and their estimated inhibitory effects on the elimination of CER in the liver in clinical situations[a]

	GEM	GEM-1-*O*-glu
C_{max}[b] (μM)	100–150	20
$1+I/IC_{50\_OATP2}$	2.4–3.1	1.8
$1+I/IC_{50\_metabolism}$	2.2–2.6	2.2
$C_{max,u}$[c] (μM)	0.65–0.97	2.3
$1+I/IC_{50\_OATP2}$	1.0	1.1
$1+I/IC_{50\_metabolism}$	1.0	1.3
$C_{max,u,liver}$[d] (μM)		81–97
$1+I/IC_{50\_metabolism}$		3.1–3.2

[a] Inhibitory effects of GEM and GEM-1-*O*-glu are represented by 1 + inhibitor concentration $(I)/IC_{50}$.
[b] Plasma concentrations of GEM and GEM-1-*O*-glu are reported by Backman et al. (2002) and Okerholm et al. (1976).
[c] Plasma unbound concentrations.
[d] Estimated unbound concentrations in the liver.

plained by its reduced renal excretion, and therefore, the effect of GEM on its elimination in the liver is weaker (Kyrklund et al., 2003). On the other hand, cyclosporin A, an inhibitor of OATP2, markedly increases the AUC of pravastatin and pitavastatin as well as CER (Regazzi et al., 1993; Hasunuma et al., 2003). The variety of effects on different statins may be due to the fact that GEM and its metabolites inhibit both the uptake and CYP2C8-mediated metabolism of CER in the liver, whereas they inhibit only the hepatic uptake of pravastatin and pitavastatin to a small extent (Table 2); on the other hand, cyclosporin A inhibits their hepatic uptake at therapeutic concentrations (Shitara et al., 2003).

In conclusion, we have shown that GEM moderately inhibits, whereas GEM-1-*O*-glu potently inhibits, the CYP2C8-mediated metabolism, and both moderately inhibit the OATP2-mediated hepatic uptake of drugs. Their inhibition of the CYP2C8-mediated metabolism of CER (mainly by GEM-1-*O*-glu concentrated in the liver) is a major mechanism that governs the clinically relevant DDI between CER and GEM, whereas their inhibition of the OATP2-mediated hepatic uptake of CER may also contribute to the DDI but to a lesser extent.

Acknowledgments

We are grateful for Bayer AG and Bayer Yakuhin for kindly providing the radiolabeled and unlabeled CER. We are also grateful for Sankyo Co., Ltd. (Tokyo, Japan) and Chemtech Labo. Inc. (Tokyo, Japan) for providing GEM-1-*O*-glu. We appreciate the generosity of Pharsight Corporation for providing a license for the computer program, WinNonlin, as part of the Pharsight Academic License (PAL) program.

References

Abdul-Ghaffar NU and El-Sonbaty MR (1995) Pancreatitis and rhabdomyolysis associated with lovastatin-gemfibrfozil therapy. *J Clin Gastroenterol* **21**:340–341.

Backman JT, Kyrklund C, Kivistö KT, Wang J-S, and Neuvonen PJ (2000) Plasma concentrations of active simvastatin acid are increased by gemfibrozil. *Clin Pharmacol Ther* **68**:122–129.

Backman JT, Kyrklund C, Neuvonen M, and Neuvonen PJ (2002) Gemfibrozil greatly increases plasma concentrations of cerivastatin. *Clin Pharmacol Ther* **72**:685–691.

Bruno-Joyce J, Dugas JM, and MacCausland OE (2001) Cerivastatin and gemfibrozil-associated rhabdomyolysis. *Ann Pharmacother* **35**:1016–1019.

Cui Y, König J, Leier I, Buchholz U, and Keppler D (2001) Hepatic uptake of bilirubin and its conjugates by the human organic anion transporter SLC21A6. *J Biol Chem* **276**:9626–9630.

Fujino H, Yamada I, Shimada S, Yoneda M, and Kojima J (2003) Metabolic fate of pitavastatin, a new inhibitor of HMG-CoA reductase: human UDP-glucuronosyltransferase enzymes involved in lactonization. *Xenobiotica* **33**:27–41.

Galetin A, Clarke SE, and Houston JB (2002) Quinidine and haloperidol as modifiers of CYP3A4 activity: multisite kinetic model approach. *Drug Metab Dispos* **30**: 1512–1522.

Galetin A, Clarke SE, and Houston JB (2003) Multisite kinetic analysis of interactions between prototypical CYP3A4 subgroup substrates: midazolam, testosterone and nifedipine. *Drug Metab Dispos* **31**:1108–1116.

Hasunuma T, Nakamura M, Yachi T, Arisawa N, Fukushima K, and Iijima H (2003) The drug-drug interactions of pitavastatin (NK-104), a novel HMG-CoA reductase inhibitor and cyclosporine. *J Clin Ther Med* **19**:381–389.

Hengy H and Kölle EU (1985) Determination of gemfibrozil in plasma by high performance liquid chromatography. *Arzneimittelforschung* **35**:1637–1639.

Hirano M, Maeda K, Shitara Y, and Sugiyama Y (2004) Contribution of OATP2 (OATP1B1) and OATP8 (OATP1B3) to the hepatic uptake of pitavastatin in humans. *J Pharmacol Exp Ther*, in press.

Hsiang B, Zhu Y, Wang Z, Wu Y, Sasseville V, Yang WP, and Kirchgessner TG (1999) A novel human hepatic organic anion transporting polypeptide (OATP2). Identification of a liver-specific human organic anion transporting polypeptide and identification of rat and human hydroxymethylglutaryl-CoA reductase inhibitor transporters. *J Biol Chem* **274**:37161–37168.

König J, Cui Y, Nies AT, and Keppler D (2000a) A novel human organic anion transporting polypeptide localized to the basolateral hepatocyte membrane. *Am J Physiol* **278**:G156–G164.

König J, Cui Y, Nies AT, and Keppler D (2000b) Localization and genomic organization of a new hepatocellular organic anion transporting polypeptide. *J Biol Chem* **275**:23161–23168.

Kyrklund C, Backman JT, Kivistö KT, Neuvonen M, Latila J, and Neuvonen PJ (2001) Plasma concentrations of active lovastatin acid are markedly increased by gemfibrozil but not by bezafibrate. *Clin Pharmacol Ther* **69**:340–345.

Kyrklund C, Backman JT, Neuvonen M, and Neuvonen PJ (2003) Gemfibrozil increases plasma pravastatin concentrations and reduces pravastatin renal clearance. *Clin Pharmacol Ther* **73**:538–544.

Mathew P, Cuddy T, Tracewell WG, and Salazar D (2004) An open-label study on the pharmacokinetics (PK) of pitavastatin (NK-104) when administered concomitantly with fenofibrate or gemfibrozil in healthy volunteers (Abstract PI-115). *Clin Pharmacol Ther* **75**:P33.

Matzno S, Tazuya-Murayama K, Tanaka H, Yasuda S, Mishima M, Uchida T, Nakabayashi T, and Matsuyama K (2003) Evaluation of the synergistic adverse effects of concomitant therapy with statins and fibrates on rhabdomyolysis. *J Pharm Pharmacol* **55**:795–802.

Moghadasian MH, Mancini GB, and Frohlich JJ (2000) Pharmacotherapy of hypercholesterolaemia: statins in clinical practice. *Expert Opin Pharmacother* **1**:683–695.

Mück W (2000) Clinical pharmacokinetics of cerivastatin. *Clin Pharmacokinet* **39**: 99–116.

Nakagawa A, Shigeta A, Iwabuchi H, Horiguchi M, Nakamura K, and Takahagi H (1991) Simultaneous determination of gemfibrozil and its metabolites in plasma and urine by a fully automated high performance liquid chromatographic system. *Biomed Chromatogr* **5**:68–73.

Nakai D, Nakagomi R, Furuta Y, Tokui T, Abe T, Ikeda T, and Nishimura K (2001) Human liver-specific organic anion transporter, LST-1, mediates uptake of pravastatin by human hepatocytes. *J Pharmacol Exp Ther* **297**:861–867.

Okerholm RA, Keeley FJ, Peterson FE, and Glazko AJ (1976) The metabolism of gemfibrozil. *Proc R Soc Med* **69 (Suppl 2)**:11–14.

Prueksaritanont T, Subramanian R, Fang X, Ma B, Qiu Y, Lin JH, Pearson PG, and Baillie TA (2002a) Glucuronidation of statins in animals and humans: a novel mechanism of statin lactonization. *Drug Metab Dispos* **30**:505–512.

Prueksaritanont T, Tang C, Qiu Y, Mu L, Subramanian R, and Lin JH (2002b) Effects of fibrates on metabolism of statins in human hepatocytes. *Drug Metab Dispos* **30**:1280–1287.

Prueksaritanont T, Zhao JJ, Ma B, Roadcap BA, Tang C, Qiu Y, Liu L, Lin JH, Pearson G, and Baillie TA (2002c) Mechanistic studies on metabolic interactions between gemfibrozil and statins. *J Pharmacol Exp Ther* **301**:1042–1051.

Regazzi MB, Campana IC, Raddato V, Lesi C, Perani G, Gavazzi A, and Vigano M (1993) Altered disposition of pravastatin following concomitant drug therapy with cyclosporin A in transplant recipients. *Transplant Proc* **25**:2732–2734.

Roca B, Calvo B, and Monferrer R (2002) Severe rhabdomyolysis and cerivastatin-gemfibrozil combination therapy. *Ann Pharmacother* **36**:730–731.

Sabordo L, Sallustio BC, Evans AM, and Nation RL (1999) Hepatic disposition of the acyl glucuronide1-O-gemfibrozil β-D-glucuronide: effects of dibromosulfophthalein on membrane transport and aglycone formation. *J Pharmacol Exp Ther* **288**:414–420.

Sabordo L, Sallustio BC, Evans AM, and Nation RL (2000) Hepatic disposition of the acyl glucuronide 1-O-gemfibrozil-β-D-glucuronide: effects of clofibric acid, acetaminophen and acetaminophen glucuronide. *J Pharmacol Exp Ther* **295**:44–50.

Sallustio BC, Fairchild BA, Shanahan K, Evans AM, and Nation RL (1996) Disposition of gemfibrozil and gemfibrozil acyl glucuronide in the rat isolated perfused liver. *Drug Metab Dispos* **24**:984–989.

Sasaki M, Suzuki H, Ito K, Abe T, and Sugiyama Y (2002) Transcellular transport of organic anions across double-transfected MDCKII cell monolayer expressing both human organic anion transporting polypeptide (OATP2/SLC21A6) and multidrug resistance associated protein 2 (MRP2/ABCC2). *J Biol Chem* **277**:6497–6503.

Shitara Y, Itoh T, Sato H, Li AP, and Sugiyama Y (2003) Inhibition of transporter-mediated hepatic uptake as a mechanism for drug-drug interaction between cerivastatin and cyclosporin A. *J Pharmacol Exp Ther* **304**:610–616.

Spence JD, Munoz CE, Hendricks L, Latchinian L, and Khouri HE (1995) Pharmacokinetics of the combination of fluvastatin and gemfibrozil. *Am J Cardiol* **76**:80A–83A.

Staffa JA, Chang J, and Green G (2002) Cerivastatin and reports of fatal rhabdomyolysis. *N Engl J Med* **346**:539–540.

Todd PA and Ward A (1988) Gemfibrozil: a review of its pharmacodynamic and pharmacokinetic properties and therapeutic use in dyslipidaemia. *Drugs* **36**:314–339.

Ueda K, Kato Y, Komatsu K, and Sugiyama Y (2001) Inhibition of biliary excretion of methotrexate by probenecid in rats: quantitative prediction of interaction from in vitro data. *J Pharmacol Exp Ther* **297**:1036–1043.

Wang J-S, Neuvonen M, Wen X, Backman JT, and Neuvonen PJ (2002) Gemfibrozil inhibits CYP2C8-mediated cerivastatin metabolism in human liver microsomes. *Drug Metab Dispos* **30**:1352–1356.

Wen X, Wang J-S, Backman JT, Kivistö KT, and Neuvonen PJ (2001) Gemfibrozil is a potent inhibitor of human cytochrome P450 2C9. *Drug Metab Dispos* **29**:1359–1361.

Wierzbicki AS, Mikhalidis DP, Wray R, Schacter M, Cramb R, Simpson WG, and Byrne CB (2003) Statin-fibrate combination: therapy for hyperlipidemia: a review. *Curr Med Res Opin* **19**:155–168.

Address correspondence to: Dr. Yuichi Sugiyama, Department of Molecular Pharmacokinetics, Graduate School of Pharmaceutical Sciences, The University of Tokyo, 7-3-1, Hongo, Bunkyo-ku, Tokyo 113-0033, Japan. E-mail: sugiyama@mol.f.u-tokyo.ac.jp

clinical situations and causes a DDI. However, it is impossible to measure the unbound concentration of CsA at the inlet to the liver and extrapolate from an in vitro inhibition study to the situation of in vivo DDI.

In the present study, to extrapolate the inhibition by CsA of the transporter-mediated uptake of CER from the in vitro to the in vivo situation, we analyzed the effect of CsA on the in vitro uptake of CER and in vivo disposition of CER in rats. Hirayama et al. (2000) examined the saturable uptake of CER in a primary culture of rat hepatocytes, and it was also taken up into human hepatocytes in a saturable manner (Shitara et al., 2003). In addition, the Oatp family transporters are conserved in rats, whereas OATP1B1 is, at least partly, responsible for the hepatic uptake of CER in humans (Shitara et al., 2003). Among the Oatps, Oatp1a1 (Oatp1), 1a4 (Oatp2), and 1b2 (Oatp4) are localized in the liver (Jacquemin et al., 1994; Noé et al., 1997; Cattori et al., 2000), although it is unknown which of them is the counterpart of OATP1B1. OATP/Oatp family transporters have similar substrate and inhibitor specificities, with some exceptions (Meier et al., 1997; Hagenbuch and Meier, 2003). In fact, CsA, an inhibitor of human OATP1B1, also inhibits rat Oatp1a1 and 1a4, although its effect on Oatp1b2 is unknown (Shitara et al., 2002). These facts suggest that the rat appears to be a good animal model for measuring the hepatic uptake of CER, although the molecular mechanisms governing the hepatic uptake in rats and humans are different. However, the metabolic profiles of CER in humans and rats are different. Both in rats and in humans, CER is mainly excreted in the form of metabolites. In humans, CER is mainly metabolized to M1 and M23, with a lesser amount of M24 by CYP2C8 and 3A4, whereas it is metabolized into many different products in rats (Mück et al., 1999; Mück, 2000; Boberg et al., 1998). Also, in rats, the isoform of cytochrome P450 responsible for its metabolism is unknown. Therefore, there is an interspecies difference between rats and humans in the molecular mechanism of the disposition and elimination of CER. However, as far as the transporter-mediated hepatic uptake is concerened, rats can be used as test models for extrapolating from in vitro to in vivo situations.

In the present study, we examined the inhibitory effect of CsA on the in vivo plasma CER concentration at steady state after intravenous administration, as well as the hepatic uptake of CER and the in vitro uptake of CER in isolated rat hepatocytes and rat Oatp1a1-expressing cells. The data obtained in the in vivo study were compared with those obtained in the in vitro study.

Materials and Methods

Reagents and Animals. [^{14}C]CER (2.03 GBq/mmol) and unlabeled CER were kindly provided by Bayer Healthcare AG (Wuppertal, Germany). CsA was purchased from Sigma-Aldrich (St. Louis, MO), and all other reagents were of analytical grade. Male Sprague-Dawley (SD) rats were purchased from Nihon SLC (Hamamatsu, Japan).

Determination of CER Plasma Concentrations in Rats. The studies were carried out in accordance with the *Guide for the Care and Use of Laboratory Animals* as adopted and promulgated by the National Institutes of Health. CER (1.32 and 4.95 μM for administration by bolus and infusion, respectively) was dissolved in saline. CsA was dissolved in a mixture of Cremophor EL (Sigma-Aldrich) and 94% ethanol (Wako, Osaka, Japan) (containing 0.65 g of Cremophor EL/ml), and subsequently diluted with 10 volumes of saline. Under light ether anesthesia, the right and left femoral veins of male SD rats weighing from 220 to 260 g were cannulated with polyethylene tubing (PE-50; BD Biosciences, Franklin Lakes, NJ). To avoid enterohepatic recirculation, which increases the inhibitor concentration in the portal vein and at the inlet to the liver, the bile duct was also cannulated with polyethylene tubing (PE-10; BD Biosciences). CER (1.32 nmol/kg) and CsA (0, 1.16, and 3.99 μmol/kg) were administered intravenously as a bolus via the right and left femoral veins, respectively, followed by infusion of CER (4.95 nmol/h/kg) and CsA (0, 0.175, and 0.599 μmol/h/kg). At 5 h after infusion, 400 μl of blood was collected from the tail vein, and EDTA (1 mg/ml) was added. At this time point, the plasma and blood concentrations of CER and CsA had both reached steady state (data not shown). The samples were stored at −20°C until analysis. Plasma concentrations of CER were determined by a validated method using atmospheric pressure ionization liquid chromatography-tandem mass spectrometry. To a 50-μl sample, 500 μl of 1 M phosphate buffer (pH 5.5) and 5 ml of diethyl ether/dichloromethane (2:1) were added; the sample was shaken for 10 min and centrifuged. Then, the organic layer was evaporated to dryness under N_2 gas at 40°C and the residue was dissolved in a 200-μl mobile phase. A 20-μl portion of each sample was then subjected to atmospheric pressure ionization liquid chromatography-tandem mass spectrometry. A Shimadzu 10A high performance liquid chromatography (HPLC) system (Shimadzu, Kyoto, Japan) combined with a model API 365 MS/MS (Applied Biosystems/MDS Sciex, Foster City, CA) equipped with a Turbo IonSpray probe was used. The analytes were separated on an Inertsil ODS-3 column (5 μm, 2.1 mm i.d.×150 mm; GL Sciences Inc., Tokyo, Japan) using a mobile phase (acetonitrile/0.2% formic acid, 60:40, v/v) at a flow rate of 0.2 ml/min. Selected reaction monitoring was used to detect the analytes and internal standard (positive mode, *m/z* 460.6/356.1). The quality control sample showed an analytical variance of less than 8.8%. Blood concentrations of CsA were determined by radioimmunoassay using CYCLO-Trac (DiaSorin, Stillwater, MN), with quality control samples that were included in the kit and confirmed the precision of assay.

Uptake of [^{14}C]CER into hepatocytes. Isolated rat hepatocytes were prepared from SD rats weighing from 220 to 250 g by the collagenase perfusion method described previously (Yamazaki et al., 1993). Isolated hepatocytes (viability >90%) were suspended in Krebs-Henseleit buffer (KHB), adjusted to 4.0×10^6 viable cells/ml, and stored on ice. Before the uptake study, hepatocytes were incubated at 37°C for 3 min and the uptake reaction was started by adding an equal volume of KHB prewarmed at 37°C containing 0.6 μM [^{14}C]CER (final concentration, 0.3 μM) with unlabeled CER or CsA. At 0.5 and 2 min, the reaction was terminated by separating the cells from the substrate solution. For this purpose, an aliquot of 100 μl of incubation mixture was collected and placed in a centrifuge tube (250 μl) containing 50 μl of 2 N NaOH under a layer of 100 μl of oil (density, 1.015; a mixture of silicone oil and mineral oil, Sigma-Aldrich), and, subsequently, the sample tube was centrifuged for 10 s using a tabletop centrifuge (10,000*g*; Beckman Microfuge E; Beckman Coulter, Fullerton, CA). During this process, the hepatocytes pass through the oil layer into the alkaline solution. After an overnight incubation at room temperature to dissolve the cells in alkali, the centrifuge tube was cut and each compartment was transferred to a scintillation vial. The compartment containing dissolved cells was neutralized with 50 μl of 2 N HCl, mixed with scintillation cocktail (Clearsol II; Nakalai Tesque, Kyoto, Japan), and the radioactivity was determined in a liquid scintillation counter (LS6000SE; Beckman Coulter). For the estimation of the inhibitory effects of CsA, it was added at the same time as [^{14}C]CER. In the present investigation, the uptake study was also conducted in incubation buffer containing 90% rat plasma to evaluate the effect of plasma protein. For this purpose, isolated hepatocytes were suspended in KHB, adjusted to 2.0×10^7 cells/ml, and prewarmed at 37°C before the uptake study. The reaction was started by addition of 9 volumes of rat plasma containing 0.25 μM [^{14}C]CER.

Uptake of CER into Rat Oatp1a1-Expressing Cells. The rat Oatp1a1-expression vector was constructed as described previously (Kouzuki et al., 1999). Rat Oatp1a1-expressing HEK293 cells and control cells were constructed by the transfection of expression vector and control pcXN2 vector, respectively, into cells using FuGENE6 (Roche Diagnostics, Indianapolis, IN), according to the manufacturer's instruction, and selection by 800 μg/ml antibiotic G418 sulfate (Promega, Madison, WI) for 3 weeks. Oatp1a1-expressing cells and control cells were cultured in Dulbecco's modified Eagle's medium (Invitrogen, Carlsbad, CA) supplemented with 10% fetal bovin serum, 1000 U/ml penicillin G sodium, 1 mg/ml streptomycin sulfate, 2.5 μg/ml amphotericin B and 200 mg/liter G418 sulfate. For the uptake study cells were seeded on 12-well plates coated with poly-L-lysine/poly-L-ornithin at 1.2×10^5 cells/well and cultured. After 2 days, culture medium wa replaced with the same culture medium containing 10 mM sodium butyrat

0090-9556/04/3212-1468–1475$20.00
DRUG METABOLISM AND DISPOSITION
Copyright © 2004 by The American Society for Pharmacology and Experimental Therapeutics
DMD 32:1468–1475, 2004

Vol. 32, No. 12
1446/1185660
Printed in U.S.A.

IN VITRO AND IN VIVO CORRELATION OF THE INHIBITORY EFFECT OF CYCLOSPORIN A ON THE TRANSPORTER-MEDIATED HEPATIC UPTAKE OF CERIVASTATIN IN RATS

Yoshihisa Shitara, Masaru Hirano, Yasuhisa Adachi, Tomoo Itoh, Hitoshi Sato, and Yuichi Sugiyama

School of Pharmaceutical Sciences, Showa University, Tokyo, Japan (Y.Sh., H.S.), Graduate School of Pharmaceutical Sciences, the University of Tokyo, Tokyo, Japan (M.H., Y.Su.); ADME/TOX Institute, Daiichi Pure Chemical, Inc., (Y.A.); and School of Pharmaceutical Sciences, Kitasato University, Tokyo, Japan (T.I.)

Received March 18, 2004; accepted September 14, 2004

This article is available online at http://dmd.aspetjournals.org

ABSTRACT:

Previously, we have shown that the inhibition of the transporter-mediated hepatic uptake of cerivastatin (CER) by cyclosporin A (CsA) could, at least partly, explain a pharmacokinetic interaction between these drugs in humans. In the present study, we have examined the effect of CsA on the in vivo disposition of CER in rats and the in vitro uptake of [^{14}C]CER in isolated rat hepatocytes in an attempt to evaluate the effect of inhibition of transporter-mediated hepatic uptake on the in vivo CER disposition. The steady-state plasma concentration of CER increased 1.4-fold when coadministered with CsA up to a steady-state blood concentration of 4 μM. Studies of [^{14}C]CER uptake into isolated rat hepatocytes showed saturable transport, with the saturable portion accounting for more than 80% of the total uptake. CsA competitively inhibited the uptake of [^{14}C]CER with a K_i of 0.3 μM. The IC_{50} for the uptake of [^{14}C]CER in the absence and presence of rat plasma was 0.2 and 2.3 μM, respectively. The in vivo hepatic uptake of [^{14}C]CER evaluated by the liver uptake index method was also inhibited by CsA in a dose-dependent manner. On the other hand, CsA did not inhibit the metabolism of [^{14}C]CER in rat microsomes. The in vitro and in vivo correlation analysis revealed that this pharmacokinetic interaction between these drugs in rats could be quantitatively explained by the inhibition of transporter-mediated hepatic uptake. Thus, this drug-drug interaction in rats is predominantly caused by the transporter-mediated uptake process.

Cerivastatin (CER) is a potent 3-hydroxy-3-methylglutaryl coenzyme A (HMG-CoA) inhibitor (statin), which was used as an effective therapeutic agent for the treatment of hypercholesterolemia (Moghadasian, 1999). However, this drug was voluntarily withdrawn from the market in 2001 due to a severe side effect, myotoxicity, which sometimes caused deaths (Charatan, 2001). Among the 31 patients who died from this side effect in the United States, 12 were concomitantly taking gemfibrozil, a fibrate (Charatan, 2001), suggesting that this side effect may be, at least partly, caused by a drug-drug interaction (DDI). Gemfibrozil has been reported to increase the area under the plasma concentration-time curve (AUC) of CER by 4- to 6-fold (Mueck et al., 2001; Backman et al., 2002). Some reports have been published claiming that this interaction is caused by inhibition of the cytochrome P450 2C8 (CYP2C8)- and uridine diphosphate glucuronosyltransferase-mediated metabolism by gemfibrozil and its metabolite (Prueksaritanont et al., 2002a,b; Wang et al., 2002; Shitara et al., 2004).

The AUC of CER was also increased when coadministered with cyclosporin A (CsA) (Mück et al., 1999). We have previously shown that this clinically relevant DDI is, at least partly, caused by the inhibition by CsA of the transporter-mediated hepatic uptake but not its metabolism (Shitara et al., 2003). CsA inhibited the transporter-mediated uptake of CER in cryopreserved human hepatocytes and in organic anion-transporting polypeptide 1B1 (OATP1B1, formerly referred to as OATP2/OATP-C)-expressing cells (Shitara et al., 2003) with the inhibition constant (K_i) of 0.2 to 0.7 μM. Although this K_i value was higher than the unbound concentration of CsA in the circulating blood in clinical situations (at most 0.1 μM), it was lower than, or similar to, the estimated maximum unbound concentration of CsA at the inlet to the liver (0.66 μM) (Ito et al., 1998a,b; Kanamitsu et al., 2000; Hirota et al., 2001). Based on this analysis, we believe that inhibition of the transporter-mediated uptake also takes place in

This study was, in part, supported by the Grant-in-Aid for Young Scientists (B) provided by the Ministry of Education, Culture, Sports, Science and Technology of Japan (Y.Sh.), Grant-in-Aid for the Advanced and Innovational Research program in Life Sciences (Y.Su.) and for the 21st Century Center of Excellence program provided by the Ministry of Education, Culture, Sports, Science and Technology, Japan (Y.Su.).

ABBREVIATIONS: CER, cerivastatin; AUC, area under the plasma concentration-time curve; CL_H, hepatic clearance; CL_{int}, intrinsic hepatic clearance; $CL_{int,all}$, overall intrinsic hepatic clearance; CL_{tot}, total body clearance; CL_{uptake}, uptake clearance; CsA, cyclosporin A; CYP2C8, cytochrome P450 2C8; DDI, drug-drug interaction; f_b, blood unbound fraction; HEK, human embryonic kidney; HPLC, high performance liquid chromatography; IC_{50}, inhibitor concentration to produce a 50% reduction in the transport; KHB, Krebs-Henseleit buffer; K_i, inhibition constant; K_m, Michaelis constant; LUI, liver uptake index; OATP/Oatp, organic anion transporting polypeptide; P_{dif}, nonsaturable uptake clearance; $PS_{u,efflux}$, membrane permeability clearance of the unbound drug for the efflux process; $PS_{u,influx}$, membrane permeability clearance of the unbound drug for the influx process; SD rat, Sprague-Dawley rat; V_{max}, maximum uptake rate.

(Wako) for the induction of Oatp1a1 expression (Schroeder et al., 1998), followed by culturing for one more day. Before the uptake study, cells were washed twice with ice-cold KHB. Then the ice-cold KHB was replaced with KHB at 37°C followed by prewarming at 37°C for 10 min. The uptake reaction was started by the replacement of KHB with a solution containing 0.3 μM [^{14}C]CER, with unlabeled CER or CsA. The reaction was terminated by removing the substrate solution by suction and, subsequently, cells were washed twice with ice-cold KHB after 5 min, since we confirmed the linearity of the uptake for at least 5 min. Cells were dissolved in 500 μl of 0.1 N NaOH overnight, followed by neutralization with 500 μl of 0.1 N HCl. Then, 800-μl aliquots were transferred to scintillation vials, and the radioactivity associated with cells and the medium was determined (LS6000SE). In addition, 50 μl of cell lysate was used for the protein assay by the Lowry method with bovine serum albumin as a standard (Lowry et al., 1951).

Protein Binding of CER in Rat Plasma. To estimate the fraction not bound to plasma protein, 3 μM [^{14}C]CER was added to rat plasma supplemented with 10% KHB and incubated for 30 min at 37°C. After that, the sample underwent ultrafiltration (Amicon Centrifree; Millipore Corporation, Bedford, MA). The radioactivity in the 90% plasma and filtrate was determined (LS6000SE) and the plasma protein unbound fraction was calculated. In a pilot study, no significant difference of protein binding was confirmed up to its concentration of 1000 μM.

Liver Uptake Index (LUI) Method. Under light ether anesthesia, the femoral vein of male SD rats (weighing from 220 to 280 g) was cannulated with polyethylene tubing (PE-50). Before the LUI study, a 2 ml/kg bolus of CsA (0, 2.4, 4.8, and 9.6 mg/kg) was administered via the femoral vein. At 5 min after intravenous administration of CsA, approximately 100 μl of blood was collected from the jugular vein for determination of the concentration of CsA. [^{14}C]CER and [^{3}H]inulin dissolved in rat plasma (approximately 18.5 and 100 kBq/ml/kg for [^{14}C]CER and [^{3}H]inulin, respectively) containing a 1:1500 dilution of CsA solution, which was used for the bolus intravenous administration, was rapidly injected into the portal vein immediately after ligation of the hepatic artery. After 18 s of bolus administration of radiolabeled compounds, which is long enough for the bolus to pass completely through the liver but short enough to prevent recirculation of the isotope (Partridge et al., 1985), the portal vein was cut and the liver was excised. The excised liver was minced, and approximately 100 mg of sample was transferred to a scintillation vial and dissolved in a solubilizing agent (Soluene-350; PerkinElmer Life and Analytical Sciences, Boston, MA) at 55°C, followed by the addition of liquid scintillation cocktail (Hionic-Fluor; PerkinElmer Life and Analytical Sciences). Also, 100 μl of injectate was transferred to a scintillation vial and liquid scintillation cocktail (Hionic-Fluor) was added. After that, the radioactivity taken up by the liver and in the injectate was determined in a liquid scintillation counter (LS6000SE).

Metabolism of CER and Testosterone in Rat Microsomes. Before the metabolism study, rat liver microsomes (final concentration 0.5 mg of protein/ml; BD Gentest, Woborn, MA) were incubated at 37°C for 10 min in 100 mM potassium phosphate buffer (pH 7.4) containing 3.3 mM $MgCl_2$, 3.3 mM glucose 6-phosphate, 0.4 U/ml glucose-6-phosphate deydrogenase, 1.3 mM NADPH, and 0.8 mM NADH. A 500- μl volume of incubation mixture was transferred to a polethyelene tube, and [^{14}C]CER (final 0.25 μM) or testosterone (final concentration 30 μM; Wako) was added to initiate the reaction with or without inhibitors. After incubation at 37°C for a designated time, the reaction was terminated by the addition of 500 μl of ice-cold acetonitrile and 20 μl of ice-cold methanol for the metabolism of [^{14}C]CER and testosterone, respectively, followed by centrifugation. To measure the metabolic rate of [^{14}C]CER, the supernatant was collected and concentrated to approximately 20 μl in a centrifugal concentrator, followed by thin-layer chromatography. The separation was carried out on a silica gel $60F_{254}$ plate (Merck, Darmstadt, Germany) using a suitable mobile phase (toluene/acetone/acetic acid, 70:30:5, v/v/v). The intensity of the bands for intact [^{14}C]CER separated by TLC was determined using the BAS 2000 system (Fuji Film, Tokyo, Japan). To measure the metabolic rate of testosterone, 6β- and 16α-hydroxytestosterone in the incubation mixture were determined by an HPLC-UV method. To a 100-μl volume of supernatant, 100 μl of internal standard (10 μg/ml phenacetin) was added followed by HPLC (VP-5 system; Shimadzu). The analyte was separated on a C18 column (Cosmosil 5C18-AR, 5 mm, 4.6 mm i.d. × 250 mm; Nakalai Tesque) at 45°C. The mobile phase consisted of a mixture of solvent A (20% tetrahydrofuran, 80% water) and solvent B (methanol). A 20-min linear gradient from 20% B to 30% B was applied at a flow rate of 1.0 ml/min. The products were detected by their absorbance at 254 nm and quantified by comparison with the absorbance of a standard curve for 6β- and 16α-hydroxytestosterone.

Data Analysis. The time courses of the uptake of [^{14}C]CER into hepatocytes were expressed as the uptake volume [μl/10^6 viable cells] for the radioactivity taken up into cells [dpm/10^6 cells] divided by the concentration of radioactivity in the incubation buffer [dpm/μl]. The initial uptake velocity of [^{14}C]CER was calculated from a slope of the uptake volume versus time plot obtained at 0.5 and 2 min and expressed as the uptake clearance (CL_{uptake}; μl/min/10^6 cells). The time courses of the uptake of [^{14}C]CER into rat Oatp1-expressing cells and vector-transfected cells were also expressed as the uptake volume (μl/mg protein) for the radioactivity in the cell lysate (dpm/mg protein) divided by the concentration of radioactivity in the incubation buffer (dpm/μl). Rat Oatp1-mediated uptake was calculated by using the uptake volume at 5 min in rat Oatp1-expressing cells and vector-transfected cells and expressed as the uptake clearance (CL_{uptake}; μl/min/mg protein), i.e., the CL_{uptake} in rat Oatp1-expressing cells minus that in vector-transfected cells.

The kinetic parameters for the uptake of [^{14}C]CER were calculated using the following equation:

$$v_0 = \frac{V_{max} \times S}{K_{m+S}} + P_{dif} \times S \quad (1)$$

where v_0 is the initial uptake rate (pmol/min/mg protein), S is the substrate concentration (μM), K_m is the Michaelis constant (μM), V_{max} is the maximum uptake rate (pmol/min/mg protein), and P_{dif} is the nonsaturable uptake clearance (μl/min/mg protein).

The uptake clearance in the isolated hepatocytes obtained in the presence of CsA was fitted to the following equation to calculate the inhibitor concentration to produce a 50% reduction (IC_{50}) in the uptake of [^{14}C]CER.

$$CL_{uptake}(+CsA) = \frac{CL_{uptake}(control) - CL_{uptake}(resistant)}{1 + I/IC_{50}} + CL_{uptake}(resistant) \quad (2)$$

where CL_{uptake}(+CsA) is the CL_{uptake} estimated in the presence of CsA, CL_{uptake}(control) is the CL_{uptake} estimated in the absence of CsA, CL_{uptake}(resistant) is the CL_{uptake} which is not affected by CsA, and I is the CsA concentration. In the presence of 90% rat plasma, these parameters were calculated based on the total concentration, not the estimated free concentration, of substrate (CER) and inhibitor (CsA). Parameters calculated based on the total concentrations of CER or CsA are referred to as $CL_{uptake,app}$, $K_{m,app}$, $P_{dif,app}$ and $IC_{50,app}$.

To determine the inhibition constant (K_i), the initial uptake rate of [^{14}C]CER into rat hepatocytes determined in the presence and absence of CsA was fitted to the following equations in which competitive inhibition was assumed:

$$v_0 = \frac{V_{max} \times S}{K_m \times \left(1 + \frac{I}{K_i}\right) + S} + P_{dif} \times S \quad (3)$$

These equations were fitted to the data obtained in the present study using a computerized version of the nonlinear least-squares method, WinNonlin (Pharsight, Mountain View, CA), to obtain the kinetic parameters or inhibition constant with a computer-calculated standard error of each estimate (computer-calculated S.E.), which means the precision of the estimated parameter, but not an estimate of inter-rat variability. The input data were weighted as the reciprocal of the observed values, and the Gauss Newton (Levenberg and Hartley) method was used as the fitting algorithm.

The data obtained in the LUI study were expressed as %LUI [%], which represents the ratio of the hepatic extraction of [^{14}C]CER to that of [^{3}H]inulin. The %LUI was obtained by the following equation:

$$\%LUI = \frac{([^{14}C]CER \text{ taken by liver}/[^{3}H]inulin \text{ taken by liver})}{([^{14}C]CER \text{ in injectate}/[^{3}H]inulin \text{ in injectate})} \times 100[\%] \quad (4)$$

where, [^{14}C]CER and [^{3}H]inulin taken up by the liver was measured based on the radioactivity associated with the liver [dpm/mg tissue] and [^{14}C]CER and

[^{3}H]inulin in the injectate were measured based on their concentrations [dpm/μl].

Statistical comparisons among multiple groups were carried out using Dunnett's test.

Results

In Vivo Study. The steady-state plasma concentrations of CER and the blood concentrations of CsA in rats 5 h after their intravenous infusion are shown in Table 1. The plasma concentration of CER significantly increased as the blood concentration of CsA increased (1.40- and 1.44-fold for 1.2 and 3.0 μM CsA; Table 1). The total body clearance (CL_{tot}) of CER was significantly reduced from 1.51 to 1.09 and 1.05 [l/h/kg] at steady-state blood concentrations of 1.2 and 3.0 μM CsA, respectively.

Uptake into Isolated Rat Hepatocytes. The uptake of CER into isolated rat hepatocytes incubated with KHB is shown in Fig. 1a. Kinetic analyses revealed that the K_m, V_{max}, and P_{dif} for the uptake of CER into isolated rat hepatocytes were 9.20 ± 2.24 μM, 1510 ± 330 pmol/min/10^6 viable cells, 35.2 ± 4.2 μl/min/10^6 viable cells (mean ± computer-calculated S.E.), respectively. The saturable component of the hepatic uptake, estimated by V_{max}/K_m, accounted for 82.4%. Uptake studies were also conducted in the presence of 90% rat plasma to investigate the effect of plasma protein binding. The apparent CL_{uptake} of CER was reduced in the presence of plasma (Fig. 1b). The kinetic parameters were 16.1 ± 2.4 μM, 481 ± 53 pmol/min/10^6 viable cells, and 2.37 ± 0.22 μl/min/10^6 viable cells (mean ± computer-calculated S.E.) for $K_{m,app}$, $V_{max,app}$, and $P_{dif,app}$, respectively (Fig. 1b). The saturable component accounted for 92.6% (Fig. 1b). Correcting for the CER-free fraction (4.32 ± 0.24%) gave unbound K_m and P_{dif} values of 0.696 μM and 0.102 μl/min/10^6 viable cells, respectively.

TABLE 1

Plasma concentration of CER and blood concentration of CsA after intravenous administration in rats

Plasma and blood concentrations of CER and CsA, respectively, were measured at 5 h after intravenous bolus injection and infusion of both compounds. All data are mean ± S.E. (n = 3–4).

Dose of CsA	Concentration of CsA	Concentration of CER
	μM	nM
0	0	3.27 ± 0.12
1.16 μmol/kg bolus injection → 0.175 mmol/h/kg infusion	1.24 ± 0.02	4.56 ± 0.52
3.99 mmol/kg bolus injection → 0.599 μmol/h/kg infusion	3.02 ± 0.22	4.71 ± 0.29**

** $p < 0.01$; a statistically significant difference from control by Dunnett's test.

Inhibition of the Uptake of [^{14}C]CER into Isolated Rat Hepatocytes by CsA. The uptake of [^{14}C]CER was examined in the presence of CsA (Fig. 2). CsA inhibited the uptake of CER into isolated rat hepatocytes in a concentration-dependent manner (Fig. 2a). The IC_{50} value was 0.198 ± 0.028 μM (mean ± computer-calculated S.E.). In the presence of 90% rat plasma, CsA inhibited the uptake of CER; however, the apparent IC_{50} values based on the total, but not free, concentration of CsA ($IC_{50,app}$) was increased. The $IC_{50,app}$ estimated in the presence of 90% rat plasma was 2.32 ± 0.33 μM (mean ± computer-calculated S.E.) (Fig. 2b). To determine the K_i value, kinetic analysis was performed in the presence of 0.1 and 0.3 μM CsA (Fig. 3). As shown in Fig. 3a, CsA affected the K_m value of CER rather than the V_{max} value, suggesting that CsA competitively inhibits the uptake of CER. This suggestion was also supported by a Lineweaver-Burk plot (Fig. 2b). Based on the competitive inhibition model (eq. 3), the K_i value of CsA was estimated to be 0.180 ± 0.023 μM (mean ± computer-calculated S.E.).

Uptake of [^{14}C]CER into Rat Oatp1a1-Expressing cells. The rat Oatp1a1-mediated uptake of [^{14}C]CER, estimated by its uptake in Oatp1a1-expressing cells minus that in control cells, is shown in Fig. 4. The K_m and V_{max} for the rat Oatp1-mediated uptake of CER were 6.42 ± 1.16 μM and 33.4 ± 4.2 pmol/min/mg protein (mean ± computer-calculated S.E.), respectively. Rat Oatp1a1-mediated uptake was also inhibited by CsA (Table 2).

LUI Study. The hepatic uptake of CER in vivo was also examined by an LUI study in rats (Fig. 5). The %LUI (eq. 4) was reduced following coadministration of CsA in a concentration-dependent manner up to 4 μM (Fig. 5). The reduction in %LUI was 66.9, 54.0, and

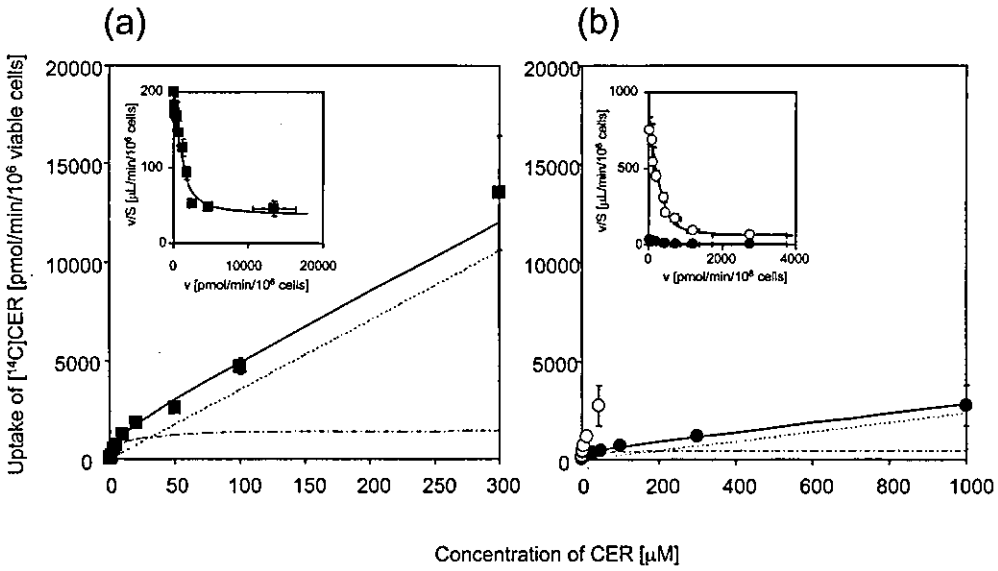

FIG. 1. The uptake of CER in isolated rat hepatocytes in the absence or presence of 90% rat plasma. Uptake of CER in isolated rat hepatocytes was examined in KHB (a) or 90% rat plasma containing KHB (b). The uptake rate versus CER concentration plot is shown. In the presence of 90% rat plasma, the data are shown with (○) and without (●) correction for CER plasma protein binding. Each point represents the mean ± S.E. (n = 3, three cell preparations). Solid lines, dotted lines, and dashed lines represent the fitted lines for total, nonsaturable, and saturable transport of CER. Eadie-Hofstee plot for the uptake of CER is also shown.

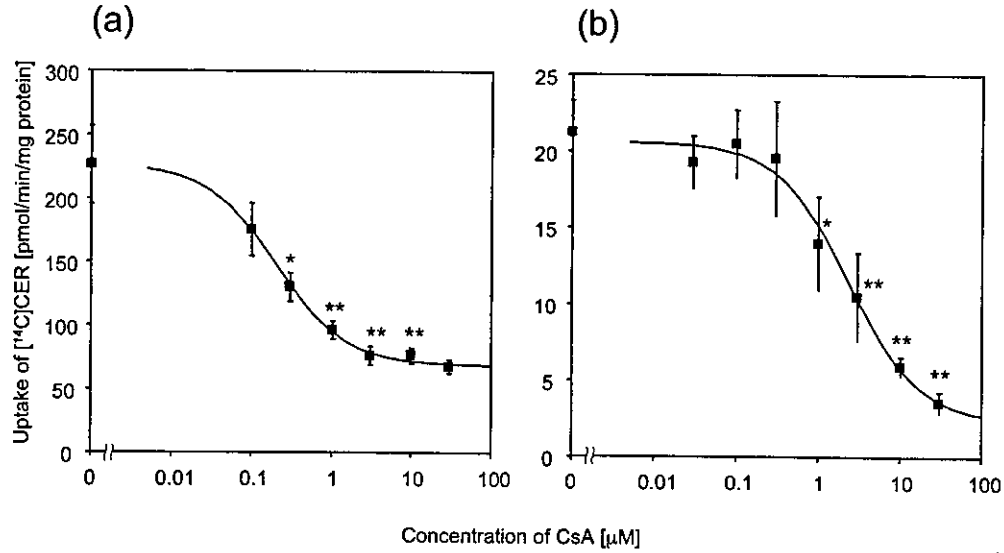

FIG. 2. Inhibitory effect of CsA on the uptake of [^{14}C]CER in isolated rat hepatocytes. The inhibitory effect of CsA on the uptake of CER (0.3 μM) in isolated rat hepatocytes was examined in the absence (a) or presence (b) of 90% rat plasma. Each point represents the mean ± S.E. (n = 3, three cell preparations). Solid lines represent the fitted lines. The asterisk represents a statistically significant difference from control shown by Dunnett's test (*, $p < 0.05$; **, $p < 0.01$).

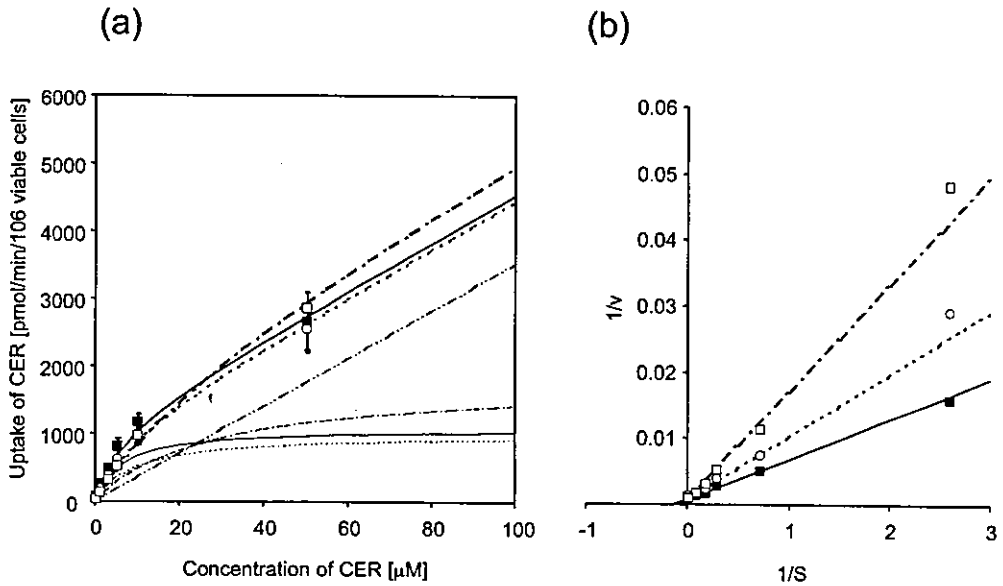

FIG. 3. The concentration-dependent uptake of CER in the presence or absence of CsA. The uptake of CER in isolated rat hepatocytes was examined in the presence of 0 (■), 0.1 (○), and 0.3 (□) μM CsA. The uptake rate versus the CER concentration plot (a) and a Lineweaver-Burk plot (b) are shown. Each symbol represents mean ± S.E. of three independent experiments. In a, thick solid, dotted, and dashed lines represent fitted curves for the total transport of CER in the presence of 0, 0.1, and 0.3 μM CsA, respectively. Thin solid, dotted, and dashed lines represent fitted curves for the saturable transport of CER in the presence of 0, 0.1, and 0.3 μM CsA, respectively. A chain double-dashed line represents the fitted curve for the nonsaturable transport of CER. In b, solid, dotted, and dashed lines represent fitted lines in the presence of 0, 0.1, and 0.3 μM CsA, respectively.

49.7% of the control for CsA blood concentrations of 2.0, 2.7, and 4.0 μM, respectively (Fig. 5).

Metabolism of [^{14}C]CER. The metabolism of [^{14}C]CER in rat microsomes was examined. After a 2 h-incubation, approximately 74% of [^{14}C]CER remained unchanged in the absence of inhibitors. The metabolism of [^{14}C]CER was not inhibited by CsA up to a concentration of 30 μM, whereas it was significantly inhibited by 0.2 μM ketoconazole (to 24.8% of the control) (Fig. 6a). The metabolism of testosterone in rat liver microsomes was also examined, and the formation rates of 6β- and 16α-hydroxylation were, respectively, 996 ± 22 and 1520 ± 10 pmol/min/mg protein (mean ± S.E.) in the absence of inhibitors (Fig. 6b). Both 6β- and 16α-hydroxylations were significantly inhibited by CsA (Fig. 6b). Ketoconazole (0.2 μM) significantly inhibited 6β-hydroxylation of testosterone, whereas it did not inhibit 16α-hydroxylation (Fig. 6b).

Discussion

The present study shows that CsA increases the plasma concentration of CER in rats in a dose-dependent manner (Table 1). It also shows that CsA inhibits the uptake of CER in rat hepatocytes, whereas it does not affect the in vitro metabolism of CER in microsomes (Figs. 2 and 6). Also in humans, CsA increases the plasma concentration of CER (Mück et al., 1999) and it potently inhibits the uptake of CER in hepatocytes with a minimal effect on the microsomal metabolism (Shitara et al., 2003). Therefore, the effect of CsA in rats appears to be similar to that in humans, although the molecular mechanisms of

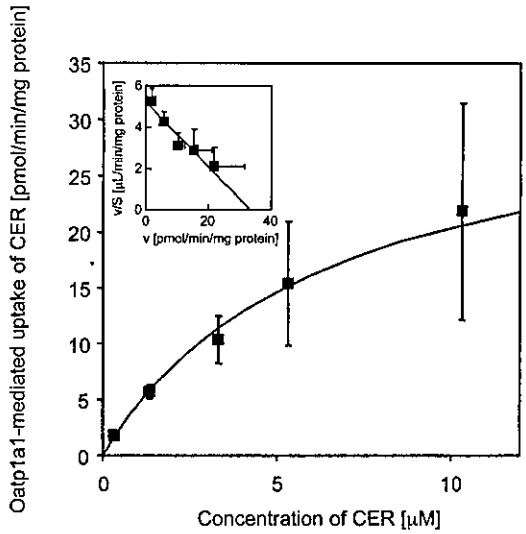

FIG. 4. The rat Oatp1a1-mediated uptake of CER. The rat Oatp1a1-mediated uptake rate of CER, which represented the uptake in Oatp1-expressing cells minus that in control cells, was plotted versus the CER concentration. Each symbol represents mean ± S.E. of three independent experiments. Solid line represents the fitted curve. The Eadie-Hofstee plot for the Oatp1a1-mediated uptake is also shown.

TABLE 2

Inhibitory effects of CsA on the Oatp1a1-mediated uptake of [^{14}C]CER

Uptake of [^{14}C]CER (0.3 μM) was observed in rat Oatp1a1-transfected and vector-transfected HEK293 cells.

Concentration of CsA	Oatp1a1-mediated uptake of [^{14}C]CER
μM	*μl/min/mg protein*
0	5.93 ± 1.01
0.1	3.66 ± 0.28**
1	3.65 ± 0.91
10	1.78 ± 0.63**

** $p < 0.01$; a statistically significant difference from control by Dunnett's test.

drug elimination in rats and humans are basically different. CsA inhibits the uptake of CER in rat hepatocytes with an unbound IC_{50} value similar to that in human hepatocytes (0.2–0.7 μM: Shitara et al., 2003). However, the in vivo effect of CsA on the disposition of CER was different between rats and humans, and the increase in the steady-state plasma concentration of CER in rats was minimal compared with that in humans. In fact, 3 μM blood CsA increased the steady-state plasma concentration of CER in rats only 1.4-fold (Table 1), whereas, in humans, CsA increased the AUC and the maximum plasma concentration of CER 3.8- and 5.0-fold, respectively, when the maximum blood concentration of CsA was approximately 1 μM (Mück et al., 1999). This difference in the severity of the interaction by these drugs between rats and humans may be explained by the different dosage regimen and experimental system. In rats, CsA, the inhibitor, was given intravenously and the biliary-excreted CsA was eliminated via cannulation without returning to the body via enterohepatic circulation, whereas, in humans, it was given orally and biliary excreted, with the CsA being transported to the portal vein and the inlet to the liver via enterohepatic circulation. In this case, the concentration of CsA at the inlet to the liver in humans may be higher than that in the circulating blood (Ito et al., 1998a,b). Therefore, in humans, a higher concentration of CsA at the inlet to the liver compared with that in the circulating blood may potently inhibit the hepatic uptake of CER, although its concentration in the circulating blood is lower in humans than in rats. However, there may be other mechanisms governing the DDI, and/or renal failure or kidney transplantation in patients may also have affected the plasma concentration of CER in the clinical case reported by Mück et al. (1999).

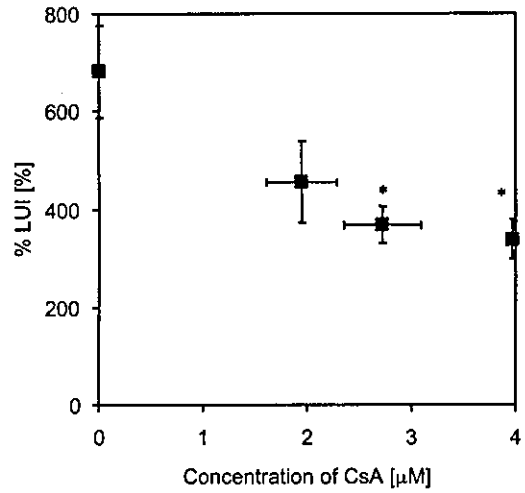

FIG. 5. Inhibitory effect of CsA on the hepatic uptake of [^{14}C]CER in rats in vivo. Inhibitory effect of CsA on the hepatic extraction of [^{14}C]CER normalized by that of [^{3}H]inulin (%LUI) during a single pass after intraportal bolus injection in rats was examined. %LUI was calculated from eq. 4. Concentration of CsA was measured just before the LUI study. Each point represents the mean ± S.E. (n = 4 and 8, with and without coadministration of CsA, respectively). The asterisk represents a statistically significant difference from control shown by Dunnett's test (*, $p <$ 0.05).

In vitro uptake studies in isolated hepatocytes revealed saturable transport of CER in rat hepatocytes both in the absence and presence of rat plasma (Fig. 1). Saturable transport of CER in primary cultured rat hepatocytes has already been reported by Hirayama et al. (2000), although their CL_{uptake} (44.4 μl/min/mg protein calculated by V_{max}/K_m) was lower than that in the present study (165 μl/min/10^6 viable cells calculated by V_{max}/K_m), assuming that 10^6 cells from our studies correspond to 1 mg of protein. This may be due to differences in the experimental system (i.e., isolated and primary cultured hepatocytes), since the transporter function can be affected by the primary culture (Ishigami et al., 1995). In the present study, we have found that the transporter-mediated uptake accounted for more than 80% and 90% of the total hepatic uptake in the absence and presence of plasma, respectively, at concentrations of CER lower than the K_m (Fig. 1). The large saturable portion of the uptake of [^{14}C]CER in hepatocytes was similar to that in humans (70–80%; Shitara et al., 2003), suggesting that transporters play an important role in the hepatic uptake and disposition of CER both in rats and humans. Kinetic parameters, i.e., K_m, V_{max}, and P_{dif}, based on the free, or estimated free, concentrations of CER were different in the presence and absence of rat plasma. This difference was due to the different range of CER free concentrations under these two sets of experimental conditions (Fig. 1).

In the present study, the Oatp1a1-mediated uptake of [^{14}C]CER was examined (Fig. 4). In our pilot studies, it was shown that other Oatp family transporters in rats, i.e., Oatp1a4 and 1b2, also accepted CER as a substrate (data not shown). However, we performed the kinetic analysis and inhibition study using CsA only in Oatp1a1-expressing cells because the highest saturable transport was observed in these cells among all the Oatp family transporter-expressing cells we possess. Kinetic analyses revealed that CER was taken up into rat Oatp1a1-expressing cells with a K_m value (6.4 μM; Fig. 3) similar to that in isolated rat hepatocytes (9.2 μM; Fig. 1). Thus, Oatp family transporter(s) appears to be responsible for the hepatic uptake of CER in rats, whereas OATP1B1, at least partly, mediates its hepatic uptake in humans (Shitara et al., 2003). The inhibition by CsA of the Oatp1a1-mediated uptake of CER was also examined (Table 2). It was